Simulating Diffusion Processes in Discontinuous Media: Benchmark Tests

Antoine Lejay, Géraldine Pichot

Simulating Diffusion Processes in Discontinuous Media: Benchmark Tests

Antoine Lejay*†‡§ Géraldine Pichot¶‖

June 10, 2014

Abstract

We present several benchmark tests for Monte Carlo methods for simulating diffusion in one-dimensional discontinuous media, such as the ones arising the geophysics and many other domains. These benchmarks tests are developed according to their physical, statistical, analytic and numerical relevance. We then perform a systematic study on four numerical methods.

Keywords. Monte Carlo methods for discontinuous media; Fick's or Darcy's law; breakthrough curve.

1 Introduction

Many diffusion models arising in geophysics, population ecology and biology for example involve second-order operators of type $\nabla(D\nabla\cdot)$, where D may be discontinuous.

Monte Carlo methods provide simple ways to solve diffusion problems. Easy to set-up and efficient (See *e.g.* [26, 44]), they are especially suitable for very large domains with complicated geometries, such as reservoir problems.

*Université de Lorraine, IECL, UMR 7502, Vandœuvre-lès-Nancy, F-54500, France

†CNRS, IECL, UMR 7502, Vandœuvre-lès-Nancy, F-54500, France

‡Inria, Villers-lès-Nancy, F-54600, France

§Contact: IECL, BP 70238, F-54506 Vandœuvre-lès-Nancy CEDEX, France. Email: `Antoine.Lejay@univ-lorraine.fr`

¶Inria, Rennes, France

‖Contact: Inria, Campus de Beaulieu, 35042 Rennes Cedex, France. Email: `Geraldine.Pichot@inria.fr`

Random walk techniques are popular in the geophysical community [57, 59]. Basically, the physical quantity of interest (pressure, concentration, ...) is approximated by averaging a suitable function over the positions of a large cloud of particles. For this, we need a rule for moving the particles during a small (deterministic or random) time step in a way which respect the physics. For linear equations, the particles move independently and their random future positions depend only on their current ones as well as on their immediate environments.

A simple technique when D is differentiable is to move during a time step δt the particle from its position x to

$$x + \xi\sqrt{2D(x)\delta t} + \nabla D(x)\delta t, \tag{1}$$

where ξ follows the unit, centered normal distribution.

This scheme no longer works when D is discontinuous (See *e.g.* [21, 31] for numerical tests). The latter case is still a challenging problem. However, the dynamic of the particles is now well understood for one-dimensional media. Many interpretations and simulation techniques have been proposed during the last twenty years. Some methods consider only the mathematical aspect of the simulation [14–16, 34, 35, 40–42] while others are driven by applications in a specific field: in geophysics [1–3, 5, 9, 12, 25, 29–31, 37, 39, 47–50, 52, 57], fluid/gas dynamics [23], ecology [8, 46, 51], brain imaging [18], astrophysics [38, 58], meteorology [56], oceanography [21, 22, 55], molecular dynamics [7, 43], ...

This article follows two goals: first, to propose benchmark tests for testing quality of numerical schemes in one-dimensional discontinuous media, with a quantification of their possible bias; second, to apply these benchmark tests on four schemes and to draw some conclusions about their quality.

Sharing benchmark tests is now a common initiative (See *e.g.* [11, 24, 27] for such initiatives with deterministic codes in geophysics). Benchmark tests for discontinuous diffusivity problems have already been dealt with in [21, 31, 51, 54]. Here, we add a statistical contribution to the benchmark tests.

A good benchmark test should be

- Physically relevant, *i.e.*, relative to a quantity of practical interest.
- Numerically relevant, *i.e.* sensitive to a quality or default of the scheme to replicate a physical phenomenon, a correct flux for example.
- Analytically relevant, *i.e.* the quantity of interest may be compared with an exact or a well approximated value.
- Statistically relevant as using empirical means over N particles leads to quantifiable fluctuations. This last point is important to discriminate the bias from the Monte Carlo error.

As we are interested in the behavior of schemes taking the discontinuities of the diffusivity into account, we consider that the diffusivity is piecewise constant over the medium. We do not consider situations where the diffusivity varies regularly not to add supplementary approximation errors. Our benchmark tests concern both the transient and the steady state regime. We propose four benchmark tests:

- LAYER:
  - Medium description: a periodic medium $[0, L]$ of diffusivity D_0, excepted on a layer of diffusivity D_m on $[L/2 - \ell, L/2 + \ell]$.
  - Test: check if the deviation from the uniform distribution is significant or not. Indeed, in the steady state regime, with periodic boundary conditions, whatever D, the particles should be uniformly distributed.
- BIMATERIAL:
  - Medium description: a medium $[0, L]$ with one interface at $x_I = L/2$ and a diffusivity D^- (resp. D^+) on $[0, x_I]$ (resp. $[x_I, L]$) and reflecting boundary conditions (BC).
  - Test: check if the proportion of particles in the right-hand side of the medium is accurate, as this quantity may be analytically computed.
- BIMATERIAL ABSORBING I & II:
  - Medium description: medium $[0, L]$ with one interface at $x_I = L/2$ and a diffusivity D^- (resp. D^+) on $[0, x_I]$ (resp. $[x_I, L]$) and a reflecting BC at 0 and an absorbing BC at L.
  - Test: check the accuracy of the loss of mass when one of the boundary is absorbing.
- SYMMETRY:
  - Medium description: same medium and same BC as BIMATERIAL.
  - Test: check whether or not the density $\mathfrak{q}(t, x, y)$, that is the density of the probability of a particle to go from x to a small volume around y during the time t, is symmetric in x and y. The more the scheme respects this property of symmetry, the better.

For this, we choose four schemes with constant time steps (our framework is not the one of Continuous Time Random Walks, which consider random time steps, see *e.g.* [39] and references within), namely,

- The exact, constant time step algorithm proposed in [32],
- The method proposed by Uffink [57],
- The method proposed by Hoteit *et al.* [25],

- A simpler version of the exact method with a linear interpolation for the time in case of crossing [32].

Outline. Theoretical results about stochastic processes are given in Section 2. The algorithms are presented in Section 3. Section 4 presents the four benchmark tests together with numerical results on the four algorithms. Some cautionary words about the size of the domain and the way to mix the schemes are given in Section 5. Finally, we expose our conclusions in Section 6.

2 Theoretical results on diffusion processes, assumptions and methods

We present very briefly the results regarding stochastic processes on which our benchmark tests are based. Diffusion processes, which are generally considered are Stochastic Differential Equations (SDE) [20, 45], are related to differential operators of type $D(y)\Delta + V(y)\nabla$. However, diffusion processes may also be associated to divergence-form operators $\nabla(D(y)\nabla\cdot)$. A large amount of known results on the links between SDE and differential operators remain true, despite they could be interpreted as solution to SDE.

2.1 Stochastic processes and Fokker-Planck equations

We consider only one-dimensional medium $[0, L]$ of finite size with periodic, reflecting or absorbing boundary conditions (BC). Hence, a medium is defined by the diffusivity D on $[0, L]$ and the BC at 0 and L.

The particles are initially distributed with a probability ν. At time t, they are distributed with a density $f(t, \cdot)$ solution to

$$\begin{cases} \partial_t f(t,y) = \nabla(D(y)\nabla f(t,y)), \\ f(t,\cdot) \xrightarrow[t\to 0]{\text{weakly}} \nu, \\ D(0)\nabla f(t,0) = D(L)\nabla f(t,L) = 0 \text{ for reflecting BC at 0 and } L, \\ \text{or } f(t,0) = f(t,L) \text{ for periodic BC}, \\ \text{or } \begin{cases} D(0)\nabla f(t,0) = 0 \\ f(t,L) = 0 \end{cases} \quad \text{for reflecting BC at 0 and absorbing BC at } L. \end{cases} \tag{2}$$

Notice this framework can be applied to many different diffusion problems by relating the particle density to the physical quantity of interest (concentration, pressure, ...).

The successive positions of the particles are appropriately defined by the paths of a stochastic process $(X_t)_{t\geq 0}$ indexed by the time on a probability space $(\Omega, \mathcal{F}, \mathbb{P})$.

The BC are taken into account in the distribution of $(X_t)_{t\geq 0}$. For example, the particle is stopped when reaching an absorbing BC.

The process follows the *Markov property*. This means roughly that for a given time $s > 0$, the distribution of $(X_t)_{t\geq s}$ of the future positions depends only on X_s and not on its prior positions $(X_r)_{r<s}$.

A numerical scheme provides us with an approximation of a path of $(X_t)_{t\geq 0}$. Justified by the Markov property, the simplest scheme consists in simulating $X_{t+\delta t}$ when X_t is known. This is a constant time step scheme. When D is smooth, the rule (1) with $x = X_t$ provides such a scheme, both simple and efficient [26, 44].

The process $(X_t)_{t\geq 0}$ is in one-to-one correspondence with a second-order differential operator. In our case, the density of X_t given $X_s = x$ for each $t > s$ is sufficient. Using time-homogeneity of the diffusivity, the density $\mathfrak{q}(t-s, x, y)$ of X_t given $X_s = x$, called the *fundamental solution* (or *Green function*) of $\nabla(D\nabla\cdot)$ is solution to the *Fokker-Planck* (or *Kolmogorov forward*) equation

$$\begin{cases} \partial_t \mathfrak{q}(t,x,y) = \nabla_y(D(y)\nabla_y \mathfrak{q}(t,x,y)), \\ \mathfrak{q}(t,x,y) \xrightarrow[t\to 0]{\text{weakly}} \delta_x(y), \\ \mathfrak{q}(t,x,\cdot) \text{ satisfies absorbing, reflecting or periodic BC.} \end{cases} \tag{3}$$

The density $f(t, y)$ solution to (2) is then equal to

$$f(t,y) = \int_0^L \nu(\,\mathrm{d}x)\mathfrak{q}(t,x,y). \tag{4}$$

The *probability current* or *flux* is $J(t, y) = -D(y)\nabla_y f(t, y)$. For each $t > 0$, $J(t, \cdot)$ is continuous over the medium, even in presence of discontinuities. At some point x_I of discontinuity of D, $J(t, x_I-) = J(t, x_I+)$ implies that

$$D(x_I-)\nabla f(t, x_I-) = D(x_I+)\nabla f(t, x_I+). \tag{5}$$

The proportion $p_{[a,b]}$ of particles in a box $[a, b] \subset [0, L]$ is $p_{[a,b]}(t) = \int_a^b f(t, y)\,\mathrm{d}y$. Integrating (2), its variation is

$$\partial_t p_{[a,b]}(t) = J(t, a) - J(t, b). \tag{6}$$

Hence, with N particles at positions $X_t^{(i)}$ at time t, $p_{[a,b]}(t)$ is easily approximated by

$$p_{[a,b]}(t) \approx \frac{1}{N}\sum_{i=1}^{N} \mathbf{1}_{[a,b]}(X_t^{(i)}). \tag{7}$$

If the BC at 0 is the same as the BC at L, then $\mathfrak{q}(t, x, y) = \mathfrak{q}(t, y, x)$ for any $t > 0$ and $x, y \in [0, L]$. Thus $x \mapsto \mathfrak{q}(t, x, y)$ also satisfies (5).

2.2 Piecewise constant diffusivity

When the diffusivity D is smooth enough and the medium is infinite, the process X is solution to the SDE $X_t = x + \int_0^t \sqrt{2D(X_s)}\,\mathrm{d}W_s + \int_0^t \nabla D(X_s)\,\mathrm{d}s$, where W is a Brownian motion. If D is discontinuous, this representation is no longer valid.

When $D = 1/2$, the stochastic process X is simply the *Brownian motion* and $\mathfrak{q}(t,x,y)$ is nothing more than the Gaussian kernel $\mathfrak{g}(t, y-x) = (2\pi t)^{-1/2}\exp(-(x-y)^2/2t)$.

With $D(x) = D^+$ if $x \geq 0$ and D^- if $x \leq 0$, the density transition function of the process X is (see *e.g.* [32, 57])

$$\mathfrak{q}(t,x,y) = \frac{1}{\sqrt{2D(y)}}\mathfrak{p}_\theta\left(t, \frac{x}{\sqrt{2D(x)}}, \frac{y}{\sqrt{2D(y)}}\right), \tag{8}$$

with

$$\theta = \frac{\sqrt{D^+} - \sqrt{D^-}}{\sqrt{D^+} + \sqrt{D^-}}. \tag{9}$$

Here $\mathfrak{p}_\theta(t,x,y)$ is the density transition function of the Skew Brownian motion of parameter θ [33] defined by

$$\mathfrak{p}_\theta(t,x,y) = \mathfrak{g}(t, y-x) + \mathrm{sgn}(y)\theta\mathfrak{g}(t, |y| + |x|).$$

In [32], we have constructed a scheme to simulate $X_{t+\delta t}$ from X_t by using (8). In a more general situation (finite media, presence of several discontinuities), there is no simple formula for the density transition function. Yet in short time, $\mathfrak{q}(\delta t, \cdot, \cdot)$ given by (8) could be used as an approximation of this density.

From the numerical point of view, the displacement of the particle during t and $t+\delta t$ is mostly influenced by the value of D close to X_t, in a region of size $\mathrm{O}(\sqrt{\delta t})$. For this reason, assuming a piecewise constant diffusivity is not restrictive at all provided that $\sqrt{\delta t}$ is small enough with respect to the distance between two discontinuities [32].

2.3 The steady-state regime: Invariant measure with periodic or reflecting BC

No mass is loss when the particle evolves on $[0, L]$ with either periodic or reflecting BC. Two facts are notable in this situation.

First, the Lebesgue measure $L^{-1}\,\mathrm{d}x$ is an *invariant measure* of the process: if the particles are uniformly distributed at initial time $t = 0$, then they remain uniformly distributed at any time $t > 0$. This case is referred to the *steady state*.

Second, the process is *ergodic* with respect to this measure. In particular, the distribution of X_t converges weakly to $L^{-1}\,\mathrm{d}x$. This will serve as the theoretical basis for the LAYER benchmark test.

We refer for example to [20] for a detailed account on these notions.

2.4 Transient regime with reflecting boundary conditions at both endpoints

We consider the case of a medium with two compartments $[0, L/2]$ and $[L/2, L]$ of respective diffusivities D^- and D^+, and two reflecting BC. We set $\rho = D^-/D^+$.

There exists a family $\lambda_0 = 0 < \lambda_1 \leq \lambda_2 \leq \cdots$ as well as a family of function $\{\phi_k\}_{k=0,1,\cdots}$ with $\phi_0(x) = 1/\sqrt{L}$ such that

$$\nabla(D\nabla\phi_k) = -\lambda_k^2\phi_k \text{ and } \int_0^L \phi_k(x)\phi_j(x)\,\mathrm{d}x = \begin{cases} 0 & \text{for } j \neq k, \\ 1 & \text{for } j = k. \end{cases}$$

The eigenvalues $-\lambda_k^2$ of the $\nabla(D\nabla\cdot)$ are given by for any $k \geq 1$,

$$\lambda_k^2 = \frac{4\,z_k^2 D^+}{L^2} \text{ with } \frac{\tan(z_k)}{\sqrt{\rho}} = -\tan\left(\frac{z_k}{\sqrt{\rho}}\right) \tag{10}$$

where $z_0 = 0 < z_1 < z_2 < \cdots$.

The eigenfunctions are

$$\phi_k(x) = \frac{1}{\kappa_k}\begin{cases} \cos\left(\alpha_k^- x\right) & \text{if } x \in [0, L/2]\,, \\ \gamma_k \cos\left(\alpha_k^+(L-x)\right) & \text{if } x \in [L/2, L]\,, \end{cases} \tag{11}$$

with

$$\alpha_k^\pm = \frac{\lambda_k}{\sqrt{D^\pm}},\ \gamma_k = \frac{\cos(\alpha_k^- L/2)}{\cos(\alpha_k^+ L/2)} \text{ and } \kappa_k^2 = \frac{L}{4}(1+\gamma_k^2) + \frac{\sin(\alpha_k^- L)}{4\alpha_k^-} + \gamma_k^2\frac{\sin(\alpha_k^+ L)}{4\alpha_k^+}.$$

For this family of eigenvalues and eigenfunctions,

$$\mathfrak{q}(t,x,y) = \frac{1}{L} + \sum_{k=1}^{+\infty} e^{-\lambda_k^2 t}\phi_k(x)\phi_k(y). \tag{12}$$

In particular, $\mathfrak{q}(t,x,\cdot)$ decreases exponentially fast to the uniform density over $[0, L]$. The value of λ_1^2 is the rate of convergence towards the steady state regime.

A tractable formula for the proportion of particles at a given time t in a volume $\mathcal{V}$ is deduced from (12) through $p_{\mathcal{V}}(t) = \int_0^L \mathrm{d}\nu(x) \int_{\mathcal{V}} \mathfrak{q}(t,x,y)\,\mathrm{d}y$. This will serve as the theoretical basis for the BIMATERIAL benchmark test.

2.5 Loss of mass with an absorbing boundary condition

We now consider a medium with two compartments $[0, L/2]$ and $[L/2, L]$ of respective diffusivities D^- and D^+, and a reflecting BC at 0 and an absorbing one at L. Again, we set $\rho = D^-/D^+$.

Let τ be the random variable that gives the first time t at which X_t reaches the absorbing boundary.

If the particles are initially distributed according to the probability ν,

$$\mathbb{P}[\tau \leq t] = 1 - \mathbb{P}[\tau > t] = 1 - \int_0^L \mathrm{d}\nu(x) \int_0^L \mathfrak{q}(t, x, y)\, \mathrm{d}y. \tag{13}$$

This quantity $\mathbb{P}[\tau > t]$ is the probability that the particle has not been absorbed before the time t. On the other hand, a spectral decomposition also holds for $\mathfrak{q}$:

$$\mathfrak{q}(t, x, y) = \sum_{k=0}^{+\infty} e^{-\widetilde{\lambda}_k^2 t} \widetilde{\phi}_k(x) \widetilde{\phi}_k(y) \text{ with } \int_0^L \widetilde{\phi}_k(x) \widetilde{\phi}_j(x)\, \mathrm{d}x = \begin{cases} 0 & \text{for } j \neq k, \\ 1 & \text{for } j = k. \end{cases} \tag{14}$$

The eigenvalues $-\widetilde{\lambda}_k^2$ are given by

$$\widetilde{\lambda}_k^2 = \frac{4\widetilde{z}_k^2 D^+}{L^2} \text{ with } \tan\left(\frac{\widetilde{z}_k}{\sqrt{\rho}}\right) = \frac{1}{\sqrt{\rho}\tan(\widetilde{z}_k)}, \tag{15}$$

where $0 < \widetilde{z}_0 < \widetilde{z}_1 < \cdots$. The corresponding eigenfunctions $\widetilde{\phi}_k$ are

$$\widetilde{\phi}_k(x) = \frac{1}{\widetilde{\kappa}_k} \begin{cases} \cos(\widetilde{\alpha}_k^- x) & \text{if } x \in [0, L/2], \\ \widetilde{\gamma}_k \sin(\widetilde{\alpha}_k^+ (L - x)) & \text{if } x \in [L/2, L], \end{cases} \tag{16}$$

with

$$\widetilde{\alpha}_k^{\pm} = \frac{\widetilde{\lambda}_k}{\sqrt{D^{\pm}}},\ \widetilde{\gamma}_k = \frac{\cos\left(\frac{\widetilde{\alpha}_k^- L}{2}\right)}{\sin\left(\frac{\widetilde{\alpha}_k^+ L}{2}\right)},\ \widetilde{\kappa}_k^2 = \frac{L}{4}(1 + \widetilde{\gamma}_k^2) + \frac{\sin\left(\widetilde{\alpha}_k^- L\right)}{4\widetilde{\alpha}_k^-} + \widetilde{\gamma}_k^2 \frac{\sin\left(\widetilde{\alpha}_k^+ L\right)}{4\widetilde{\alpha}_k^+}.$$

All the eigenvalues have multiplicity 1 and $\widetilde{\lambda}_0 \neq 0$. The eigenfunction $\widetilde{\phi}_0$ never vanishes in $(0, L)$. Hence $\mathfrak{q}(t, x, y)$ is exponentially fast decreasing and

$$\mathbb{P}[\tau \leq t] \approx 1 - \widetilde{\kappa} e^{-\widetilde{\lambda}_0^2 t} \text{ with } \widetilde{\kappa} = \int_0^L \mathrm{d}\nu(x) \int_0^L \widetilde{\phi}_0(x) \widetilde{\phi}_0(y)\, \mathrm{d}y. \tag{17}$$

This will serve as the theoretical basis for the BIMATERIAL ABSORBING I & II benchmark tests.

2.6 Significance tests

Monte Carlo simulations are justified by the law of large numbers. One relates the quantity of interest to an averaged quantity.

Using a finite number of particles in (7) induces an error, called the *Monte Carlo error*, that cannot be avoided and which is in general of order $\mathrm{O}(N^{-1/2})$.

However, an approximation scheme may induced an error, called the *bias*, which we are interested in quantifying. The smaller, the better. However, the bias may be small in front of the Monte Carlo error.

A part of our methodology relies on the theory of *significance tests* (See *e.g.* [19, Chap. 12] or [10]). The benchmark tests we propose consist in approximating some quantities in a way we may quantify the Monte Carlo error when the scheme is assumed to have no bias (this is the *null hypothesis*). A test is *passed* if one cannot distinguish the bias from the Monte Carlo error. Otherwise the test *failed*. This procedure is partially subjective for two reasons. First, a confidence level should be defined by the user. Second, if a test failed, the user may decide that a bias is induced by the scheme. Yet a passed test does not mean at all that the scheme is bias-free. And a failed test could be attributed to an exceptional realization under the null hypothesis.

To be more precise, we estimate the distance between a value Λ and an empirical quantities Λ_N (resp. $\overline{\Lambda}_N$) constructed using N particle moving according to the true dynamics (resp. the scheme). Typically, $\Lambda = p_{\mathcal{V}}(t) = \mathbb{P}[X_t \in \mathcal{V}]$ for a volume $\mathcal{V}$, and $\overline{\Lambda}_N = N^{-1}\#\{i; \overline{X}_t^{(i)} \in \mathcal{V}\}$ for N independent realizations of the positions of the particles moving according to one of the schemes.

We place ourselves in situation where thanks to the Central Limit Theorem, for N large enough, $\sqrt{N}(\Lambda_N - \Lambda)$ is close in distribution to κG for a constant κ and G is a unit, centered normal distribution $\mathcal{N}(0,1)$. We fix a confidence level α close to 1 and we set d_α so that

$$\mathbb{P}[G \in [-d_\alpha, d_\alpha]] = \alpha. \tag{18}$$

To draw a conclusion from our test, we then compare $\sqrt{N}|\overline{\Lambda}_N - \Lambda|$ with κd_α. We use for $\alpha = 99\,\%$, so that $d_\alpha = 2.57$. When $\Lambda(t)$ and $\kappa(t)$ depend on a parameter t, $t \mapsto \pm\kappa(t)d_\alpha$ is called a *confidence band*.

In the several situations we consider, alternative statistical tests could be constructed. However, for the sake of simplicity, we prefer to use this simple procedure which we combine with a graphical approach.

3 Algorithms

3.1 Three zones

We define three kind of zones (See Figure 1):

- The interface layer I_{layer}, around a discontinuity at x_I,
- The boundary layer,
- The constant diffusivity zone.

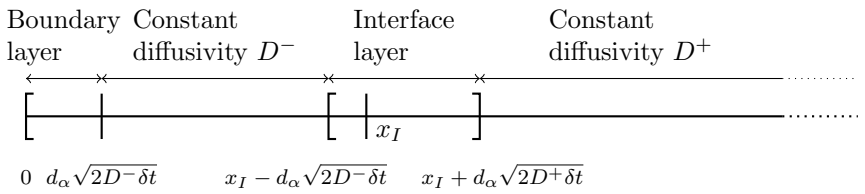

Figure 1: Three kind of zones: interface layer, boundary layer, zone of constant diffusivity

The particles are moved with a constant time step δt.

For a discontinuity at the position x_I, the interface layer is: $I_{\text{layer}}(x_I) = [x_I - d_\alpha\sqrt{2D^-\delta t}, x_I + d_\alpha\sqrt{2D^+\delta t}]$, with $\mathbb{P}[|G| \leq d_\alpha] = \alpha$ for $G \sim \mathcal{N}(0,1)$. We choose $d_\alpha = 4$, corresponding to $\alpha = 1 - 6 \times 10^{-5} = 99.994\,\%$.

The particle is within the *boundary layer* if it is at the distance lower than $d_\alpha\sqrt{2D^\pm\delta t}$ from it.

This means that, when a particle is at distance greater than $d_\alpha\sqrt{2D^\pm\delta t}$ from an interface or a boundary, it reaches it a very low probability so that we act as if the diffusivity is constant. This defines the zone of *constant diffusivity*.

3.2 Algorithms in the constant diffusivity zone

In the zone of *constant diffusivity*, we use Gaussian (See Algorithm 1) or Uniform steps (See Algorithm 2).

Data: The position x of the particle at time t, a time step δt and a diffusivity D.
Result: The position $X_{t+\delta t}$ at time $t + \delta t$ of the particle.
Draw a random variate $\xi \sim \mathcal{N}(0,1)$;
return $x + \sqrt{2D\delta t}\xi$;

Algorithm 1: `GaussianStep`$(x, \delta t, D)$: Gaussian step in a zone of constant diffusivity D.

Data: The position x at time t of the particle, a time step δt and a diffusivity D.
Result: The position $X_{t+\delta t}$ at time $t+\delta t$ of the particle.
Draw a random variate $U \sim \mathcal{U}(0,1)$;
return $x + \sqrt{6D\delta t}(2U-1)$;

Algorithm 2: `UniformStep`$(x, \delta t, D)$: Uniform step in a zone of constant diffusivity D.

3.3 Algorithms in the boundary layer

In the *boundary layer*, the hitting time may be computed either exactly (see Algorithm 3: `ExactHittingTime`) or with a linear approximation (see Algorithm 4: `LinearHittingTimeUS` and `LinearHittingTimeGS`).

3.4 Algorithms in the interface layer

In the intervals $I_{\text{layer}}(x_I)$ around each interface with position x_I, we only apply one of the four specific schemes, `SBM`, `Uffink`, `Hoteit` or `SBMlin`.

We consider four algorithms:

- `SBM`: The exact, constant time step algorithm proposed in [32] (We warn that a normalization factor 1/2 has been added for convenience in this reference in front of the diffusivity coefficient), see Algorithm 5.
- `Uffink`: The method proposed by Uffink [57], see Algorithm 6.
- `Hoteit`: The method proposed by Hoteit *et al.* [25], see Algorithm 7.
- `SBMlin`: A simpler version of the exact method, with a linear interpolation for the time in case of crossing [32], see Algorithm 5.

Figure 2 presents the density $\overline{\mathfrak{q}}(\delta t, x, \cdot)$ of the schemes after one step $\delta t = 0.01$ for three values of x in a medium with a diffusivity $D^- = 5$ on $[0,2]$ and $D^+ = 0.5$ on $(2,4]$ and reflecting boundary conditions (such a medium will be referred as a bimaterial one, see Section 4.2).

From now, each method is associated to a color using the correspondence given in Table 1.

3.5 Combination of algorithms in the whole domain

For each particle, we generate a random sequence $\{\overline{X}_{k\delta t}\}_{k=0,1,2,\dots}$ of approximations of $\{X_{k\delta t}\}_{k=0,1,2,\dots}$. For this, $\overline{X}_{k\delta t}$ depends only on $\overline{X}_{(k-1)\delta t}$ according to a density $\overline{\mathfrak{q}}(\delta t, \overline{X}_{(k-1)\delta t}, \cdot)$, where $\overline{\mathfrak{q}}$ is an approximation of $\mathfrak{q}$.

Table 2 summarizes the combinations of algorithms for dealing with the whole medium according to the zone (interface layer, boundary layer, zone of constant diffusivity: See Figure 1) in which the particle is. See Section 5.2 for a rationale for this choice of combination.

Data: The position x at time t of the particle, a time step δt and a diffusivity D.
Result: The position (s, X_s) which is either $(\tau, 0)$ if $\tau < t + \delta t$ or $(t + \delta t, X_{t+\delta t})$, where $\tau = \inf\{s > t; X_s = 0\}$.
Draw a random variate $\xi \sim \mathcal{N}(0, 1)$;
Set $z \leftarrow x/\sqrt{2D}$; `/* Normalize the position */`
Set $y \leftarrow z + \sqrt{\delta t}\xi$; `/* Try a first guess */`
if $\mathrm{sgn}(z) \neq \mathrm{sgn}(y)$ **then**
  `/* The boundary/interface has been crossed. */`
  Generate a random variate $\xi \sim \mathcal{IG}(|z|/|y|, z^2/\delta t)$;
  Set $\tau \leftarrow \delta t \times \xi/(1 + \xi) + t$;
  return $(\tau, 0)$;
else
  `/* Check if the boundary/interface has been crossed. */`
  Generate a random variate $\xi \sim \mathcal{IG}(|z|/|y|, z^2/\delta t)$;
  Generate a random variate $U \sim \mathcal{U}(0, 1)$;
  if $U < \exp(-2zy/\delta t)$ **then**
    `/* The boundary/interface has been crossed. */`
    Generate a random variate $\xi \sim \mathcal{IG}(|z|/|y|, z^2/\delta t)$;
    Set $\tau \leftarrow \delta t \times \xi/(1 + \xi) + t$;
    return $(\tau, 0)$;
  else
    `/* The boundary/interface has not been crossed. */`
    return $(t + \delta t, y\sqrt{2D})$;
  end
end

Algorithm 3: `ExactHittingTime`$(t, x, \delta t, D)$: Exact simulation of the first hitting time of 0, where $\mathcal{IG}(\alpha, \beta)$ is the inverse Gaussian distribution of parameters (α, β) (See *e.g.* [32]).

Data: The position x at time t of the particle, a time step δt and a diffusivity D.
Result: The position (s, X_s) which is either $(\tau, 0)$ if $\tau < t + \delta t$ or $(t + \delta t, X_{t+\delta_t})$, where τ is an approximation of $\inf\{s > t; X_s = 0\}$
Draw a new position y according to `GaussianStep` $(x, \delta t, D)$ or to `UniformStep` $(x, \delta t, D)$;
if $\mathrm{sgn}(x) \neq \mathrm{sgn}(y)$ **then**
  `/* The boundary/interface has been crossed. */`
  Set $\tau \leftarrow \delta t \frac{|x|}{|x|+|y|} + t$;
  return $(\tau, 0)$
else
  `/* The boundary/interface has not been crossed. */`
  return $(t + \delta t, y)$
end

Algorithm 4: `LinearHittingTimeUS`$(t, x, \delta t, D)$ and `LinearHittingTimeGS`$(t, x, \delta t, D)$: Linear approximation of the first hitting time of 0 with a Uniform Step (US) or a Gaussian Step (GS).

Data: An initial position $X_t = x$ and a time $\delta t > 0$ in the interface layer $I_{\text{layer}}(x_I)$ of an interface at x_I.
Result: A position of $X_{t+\delta t}$ according to the SBM algorithm.
(SBM) Set $(s, y) \leftarrow$ `ExactHittingTime` $(t, x - x_I, \delta t, D^{\text{sgn}(x-x_I)})$
(SBMlin) Set $(s, y) \leftarrow$ `LinearHittingTimeGS` $(t, x - x_I, \delta t, D^{\text{sgn}(x-x_I)})$
if $s < t + \delta t$ **then**
  `/* A crossing occurred: biased step */`
  Generate a random variate $U \in\sim \mathcal{U}(0, 1)$;
  Generate a random variate $G_2 \sim \mathcal{N}(0, 1)$;
  if $U < (1 + \theta)/2$ **then**
    return $x_I + \sqrt{2D^+(t + \delta t - s)}|G_2|$
  else
    return $x_I - \sqrt{2D^-(t + \delta t - s)}|G_2|$
  end
else
  `/* No crossing occurred */`
  return $x_I + y$
end

Algorithm 5: `SBM` and `SBMlin` algorithms with the two-steps method.

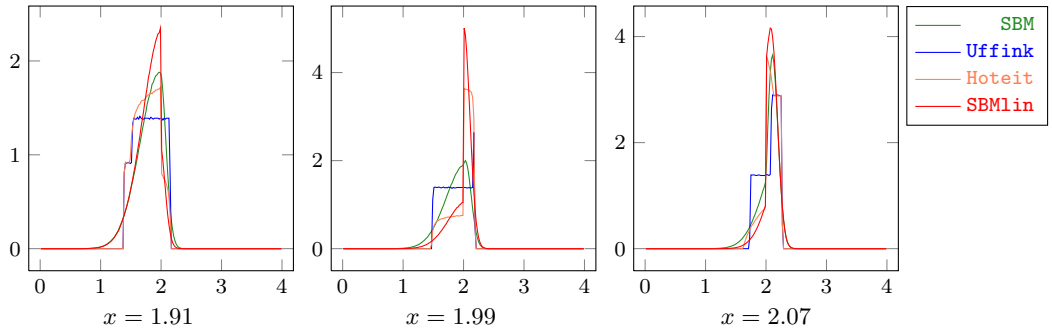

Figure 2: Densities of the schemes after one step $\delta t = 0.01$ in a discontinuous medium for different starting points close to the interface located at 2.

4 Benchmark tests

We simulate the dynamic of N particles until the final time T is reached.

We consider four benchmark tests:

- LAYER: a periodic medium $[0, L]$ of diffusivity D_0, excepted on a layer of diffusivity D_m on $[L/2 - \ell, L/2 + \ell]$.
- BIMATERIAL: a medium $[0, L]$ with one interface at $x_I = L/2$ and a diffusivity D^- (resp. D^+) on $[0, x_I]$ (resp. $[x_I, L]$) and reflecting boundary conditions (BC).
- BIMATERIAL ABSORBING: medium $[0, L]$ with one interface at $x_I = L/2$ and

Data: An initial position $X_t = x$ and a time step $\delta t > 0$ in the interface layer $I_{\text{layer}}(x_I)$ of an interface at x_I
Result: A position $X_{t+\delta t}$ according to Uffink's algorithm
Compute $H_1 = \sqrt{D^- \, 6 \, \delta t}$ and $H_2 = \sqrt{D^+ \, 6 \, \delta t}$;
Set $z \leftarrow x - x_I$; `/* Shift the position */`
if $z + H_1 < 0$ **then**
  `/* the interface is not crossed: uniform step */`
  Generate a random variate $V \sim \mathcal{U}(0,1)$;
  return $z + (2V - 1)H_1$
else
  if $z < 0$ **then**
    `/* The interface is crossed: compute` P_H `*/`
    Compute $x_L = z - H_1$, $x_M = -z - H_1$ and $x_R = (x + H_1)\,\dfrac{H_2}{H_1}$;
    Compute $P_H = \dfrac{1}{2\,H_1}(x_M - x_L)$;
  else
    if $z - H_2 > 0$ **then**
      `/* the interface is not crossed: uniform step */`
      Generate a random variate $V \sim \mathcal{U}(0,1)$;
      return $x + (2V - 1)H_2$
    else
      `/* The interface is crossed: compute` P_H `*/`
      Compute $x_L = x + (z - H_2)\,\dfrac{H_1}{H_2}$, $x_M = x_I - (z - H_2)$ and $x_R = x + H_2$;
      Compute $P_H = \dfrac{(1+\theta)}{2\,H_2}(x_M - x_L)$ with θ given by Eq. (9);
    end
  end
end
`/* The interface is crossed: biased step */`
Generate a random variate $U \sim \mathcal{U}(0,1)$;
Generate a random variate $V \sim \mathcal{U}(0,1)$;
if $U \leq P_H$ **then**
  return $x_L + (x_M - x_L)\,V$
else
  return $x_M + (x_R - x_M)\,V$
end

Algorithm 6: `Uffink` algorithm.

Data: An initial position $X_t = x$ and a time $\delta t > 0$ in the interface layer $I_{\text{layer}}(x_I)$ of an interface at x_I.
Result: A position $X_{t+\delta t}$ according to Hoteit's algorithm
Compute $H_1 = \sqrt{D^- 6\,\delta t}$ and $U_2 = \sqrt{D^+ 6\,\delta t}$;
Set $z \leftarrow x - x_I$; `/* Shift the position */`
Set $(s, z_{\text{next}}) \leftarrow$ `LinearHittingTimeUS` $(t, z, \delta t, D^{\text{sgn}(z)})$;
if $s < t + \delta t$ **then**
  `/* The interface is crossed: biased step */`
  `/* Time splitting */`
  Compute $\delta t_2 = \delta t - s$;
  Generate a random variate $U \sim \mathcal{U}(0,1)$;
  if $U < \dfrac{1-\theta}{2}$ **then**
    Compute $x_L = x_I - \sqrt{D^- 6\,\delta t_2}$;
    Set $x_R = x_I$;
  else
    Set $x_L = x_I$;
    Compute $x_R = x_I + \sqrt{D^+ 6\,\delta t_2}$;
  end
  Generate a random variate $W \sim \mathcal{U}(0,1)$;
  return $x_L + (x_R - x_L)\,W$;
else
  `/* The interface is not crossed: uniform step */`
  return $x_I + z_{\text{next}}$
end

Algorithm 7: `Hoteit` algorithm.

`SBM`	⇝ Green	`Hoteit`	⇝ Coral
`Uffink`	⇝ Blue	`SBMlin`	⇝ Red

Table 1: Color convention for the schemes.

- Interface layer
  - ⋆ `SBM`: see Algorithm 5.
  - ⋆ `Uffink`: see Algorithm 6.
  - ⋆ `Hoteit`: see Algorithm 7.
  - ⋆ `SBMlin`: see Algorithm 5.
- Boundary layer
  - ⋆ absorbing
    - – `ExactHittingTime` (with `SBM`): See Algorithm 3.
    - – `LinearHittingTimeUS` (with `Uffink` or `Hoteit`). See Algorithm 4.
    - – `LinearHittingTimeGS` (with `SBMlin`). See Algorithm 4.
  - ⋆ periodic: reinject the particle into the medium in a periodic way.
  - ⋆ reflecting: perform a reflection around the boundary point.
- Zone of constant diffusivities.
  - ⋆ `GaussianStep` (with `SBM` or `SBMlin`): See Algorithm 1.
  - ⋆ `UniformStep` (with `Uffink` or `Hoteit`): See Algorithm 2.

Table 2: Combination of the algorithms for the three kinds of zone.

a diffusivity D^- (resp. D^+) on $[0, x_I]$ (resp. $[x_I, L]$) and a reflecting BC at 0 and an absorbing BC at L

- Symmetry: same conditions as Bimaterial.

The parameters we use are given in Table 3.

4.1 Layer benchmark test: check the distribution of the particles in the steady state regime

In this benchmark test, we check if the particles remain uniformly distributed after many steps in the steady state regime.

	Layer	Bimaterial	Bimaterial absorbing	Symmetry
L	$L = 3$; $\ell = 0.5$	$L = 2$	$L = 2$	$L = 4$
BC	periodic	reflecting/reflecting	reflecting/absorbing	reflecting/reflecting
X_0	uniform	1.5	0.1	$(i + 1/2) \times L/200$
D	$\begin{cases} D_0 = 5 \\ D_m = D_0/\rho \end{cases}$	$\begin{cases} D^- = 5 \\ D^+ = D^-/\rho \end{cases}$	$\begin{cases} D^- = 5 \\ D^+ = D^-/\rho \end{cases}$	$\begin{cases} D^- = 5 \\ D^+ = 1/3 \end{cases}$
ρ	$[2.5 : 750]$	$\begin{array}{c\|c\|c\|c} [2.5:20] & 100 & [250:500] & 750 \\ 15 & 100 & 300 & 400 \end{array}$	$\begin{array}{c\|c\|c\|c\|c\|c} [2.5:20] & 100 & 250 & 500 & 750 \\ 100 & 250 & 750 & 1500 & 2000 \end{array}$	15
T	10			0.2
δt	0.001	0.001	0.001	0.01
N	2×10^6	4×10^6	2×10^6	2×10^6
ρ	$\{2.5, 5, 7.5, 10, 12.5, 15, 17.5, 20, 100, 250, 500, 750\}$			

Table 3: Parameters for the benchmark tests.

4.1.1 LAYER: Description

As seen in Section 2.3, the Lebesgue measure is an invariant measure for the particles when periodic or reflecting BC are enforced in a finite size medium. Thus, if the particles are initially uniformly distributed over the medium, they should remain uniformly distributed as the time evolves, whatever the number of interfaces.

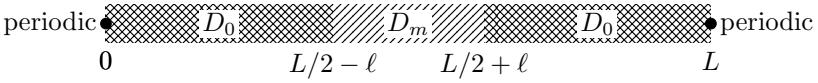

Figure 3: Medium for the LAYER test.

We consider a periodic medium $[0, L]$ of diffusivity D_0, excepted on a layer of diffusivity D_m on $[L/2 - \ell, L/2 + \ell]$ (see Figure 3).

Denote by X_t (resp. $\overline{X}_t$) the position of the particles at time t moved with the real dynamics (resp. when one of the scheme is used), and by $X_t^{(i)}$ (resp. $\overline{X}_t^{(i)}$) the position at time t of the i-th particle moved with the real dynamics (resp. when one of the scheme is used) when N independent particles paths are drawn.

The empirical distribution functions of X_t/L and $\overline{X}_t/L$ are, for $y \in [0, 1]$:

$$F_N(t, y) = \frac{1}{N} \sum_{i=1}^{N} \mathbf{1}_{X_t^{(i)} \leq Ly} \text{ and } \overline{F}_N(t, y) = \frac{1}{N} \sum_{i=1}^{N} \mathbf{1}_{\overline{X}_t^{(i)} \leq Ly}. \tag{19}$$

The distribution functions of X_t/L and $\overline{X}_t/L$ are, for $y \in [0, 1]$,

$$F(t, y) = \mathbb{P}[X_t \leq Ly] = \mathbb{E}[F_N(t, y)] \text{ and } \overline{F}(t, y) = \mathbb{P}[\overline{X}_t \leq Ly] = \mathbb{E}[\overline{F}_N(t, y)].$$

If the the scheme is bias-free, then $\overline{F}(t, y) = F(t, y)$. Yet $\overline{F}(t, y)$ is only known through its empirical approximation $\overline{F}_N(t, y)$.

The Glivenko-Cantelli theorem states that $F_N(t, y) \xrightarrow[N\to\infty]{} F(t, y)$ for any $y \in [0, 1]$ (See [19, 53]). Moreover, $F_N(t, y)$ follows a binomial distribution and

$$\sqrt{N}(F_N(t, y) - y) \xrightarrow[N\to\infty]{\text{law}} B_b(F(t, y)) \text{ for } y \in [0, 1], \tag{20}$$

where B_b is a Brownian bridge on $[0, 1]$ with $B_b(0) = B_b(1) = 0$. For each $t > 0$ and $x \in [0, 1]$, $B_b(F(t, x))$ follows the Gaussian distribution with mean 0 and variance $F(t, x)(1 - F(t, x))$. This means in particular that for $\alpha \in (0, 1)$,

$$\mathbb{P}\big[B_b(y) \in [-d_\alpha \sqrt{y(1-y)}, d_\alpha \sqrt{y(1-y)}]\big] = \alpha, \tag{21}$$

where d_α is defined by (18).

4.1.2 LAYER: Benchmark test definition

As the uniform distribution is an invariant measure for the process X, if $X_0 \sim \mathcal{U}(0, L)$, then $X_t \sim \mathcal{U}(0, L)$ so that $F(t, y) = y$ for any $y \in [0, 1]$.

We test for t large enough (hence after many steps) the deviation of $\overline{F}_N(t, \cdot)$ from $F(t, \cdot)$ when the N particles are uniformly distributed at $t = 0$. For this, we use the convergence (20) and the control (21) on the marginals of the Brownian bridge.

The statistic of interest is

$$K_N(t, y) = \sqrt{N}(\overline{F}_N(t, y) - y). \tag{22}$$

The *null hypothesis* is that $\overline{F}_N(t, y)$ is a realization of $F(t, y) = y$ for any $y \in [0, 1]$. Under this hypothesis, (20) implies that $K_N(t, y)$ converges to a Brownian bridge.

Among the many ways to check the deviation of $\overline{F}_N(t, y)$ from y, the popular Kolmogorov-Smirnov test relies on comparing the supremum of $|K_N(t, \cdot)|$ with the one of a Brownian bridge [17, 19, 53]. The Kuiper test provides an alternative to this test, where the quantity of interest is the maximum of $\sup \max\{K_N(t, \cdot), 0\}$ and $\sup \max\{-K_N(t, \cdot), 0\}$. This test is best adapted for periodic medium [28].

We prefer a more graphical procedure relying on (21) and (22), and normal confidence intervals. With this approach, the correlations between $\overline{F}_N(t, x)$ and $\overline{F}_N(t, y)$ for $x \neq y$ are not taken into account. However, this test is very simple to set up and allows one to see where the bias of the schemes take their effect, if any.

LAYER. For a time t large enough, plot $K_N(t, y)$ and compare it with $y \in [0, 1] \mapsto \pm d_\alpha \sqrt{y(1 - y)}$ for a confidence level α.

This benchmark test is sensitive to the capacity of the numerical scheme to preserve the symmetry condition $\mathfrak{q}(\delta t, x, y) = \mathfrak{q}(\delta t, y, x)$ for any $x, y \in [0, L]$. As such, it is not restricted to this particular medium, and may be applied to media containing several layers for example.

4.1.3 LAYER: Numerical results

In Figure 4, we plot $K_N(t, \cdot)$ defined by (22) for the values of $\rho = D_0/D_m$ given by Table 3.

`SMBlin` method fails in preserving the uniform distribution of the particles with time. On the contrary, `SBM`, `Uffink` and `Hoteit` methods pass this test.

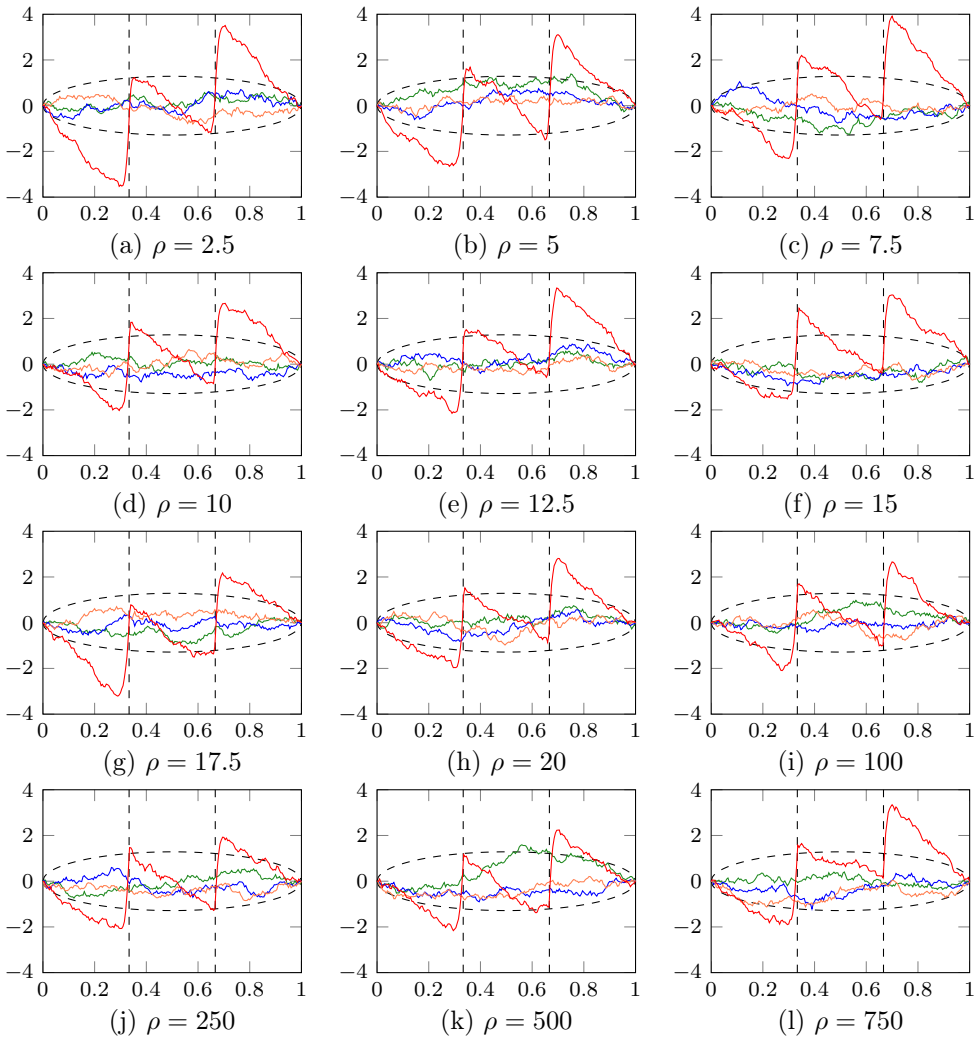

Figure 4: LAYER — Plot of $x \mapsto K_N(t,x)$ for the four methods: SBM, Uffink, Hoteit and SBMlin and comparison with the 99 %-confidence band $y \mapsto \pm d_{0.99}\sqrt{y(1-y)}$ at $T = 10$.

4.2 BIMATERIAL benchmark tests: check the proportions of particles on each side of the interface in the steady state and transient regime

The second benchmark test checks the preservation of the flux condition (5) at the interface.

This benchmark test is a refinement of the one proposed by E. Labolle *et al.* [31]. It could be adapted to more general media, for example with multiple compartments.

4.2.1 BIMATERIAL: Description

The proportion of particles in $\mathcal{V}$ is the integral of the solution $f(t,x)$ to (2) over $\mathcal{V}$.

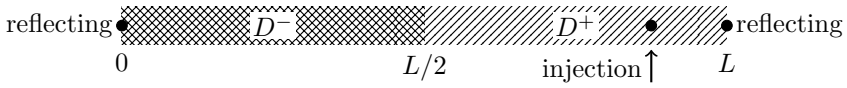

Figure 5: Medium for the BIMATERIAL test.

We consider a medium $[0, L]$ with one interface at $x_I = L/2$ and reflecting BC (See Figure 5). The diffusivity is D^- (resp. D^+) on $[0, x_I]$ (resp. $[x_I, L]$). The particles start from an injection point at x with an initial mass equal to 1. At time t, the proportion of particles on $[0, x_I]$ (resp. $[x_I, L]$) follows from (4) so that

$$p_-(t) = p_{[0,L/2]}(t) = \int_0^{x_I} f(t,y)\,\mathrm{d}y = \int_0^{x_I} \mathfrak{q}(t,x,y)\,\mathrm{d}y$$
$$\text{resp. } p_+(t) = p_{[L/2,L]}(t) = \int_{x_I}^{L} f(t,y)\,\mathrm{d}y = \int_{x_I}^{L} \mathfrak{q}(t,x,y)\,\mathrm{d}y.$$

The spectral decomposition (12) of $\mathfrak{q}$ gives an analytic expression for the proportion of particles. In particular, after a short time, $p_\pm(t)$ converges to $1/2$ (since $x_I = L/2$) at time exponential rate $-\lambda_1^2$.

With (6), a scheme which respect well the flux $J(t, y\pm)$ should lead to a correct variation of $p_\pm(t)$.

Using (7), the idea of this benchmark is then to compare the theoretical evolution of $p_+(t)$ with the proportion of particles on the right-hand side of the medium.

In [31], it is shown that the repartition of masses is not correct if a simple Gaussian random walk is used. In the latter case, the gradient of f is continuous at the interface, not its flux.

4.2.2 BIMATERIAL: Benchmark test definition

We let N particles, starting from a fixed point, evolve in the medium with reflecting boundary conditions, by using one of the schemes. The position of the i-th particle at time t is denoted by $\overline{X}_t^{(i)}$. This is an approximation of $X_t^{(i)}$, the position of the i-th particle at time t which follows the real dynamics.

The statistics of interest are:

$$P_N(t) = \frac{1}{N}\sum_{i=1}^{N} \mathbf{1}_{X_t^{(i)} \geq L/2} \text{ and } \overline{P}_N(t) = \frac{1}{N}\sum_{i=1}^{N} \mathbf{1}_{\overline{X}_t^{(i)} \geq L/2}. \tag{23}$$

ρ	2.5	5	7.5	10	12.5	15	17.5	20	100	250	500	750
z_1	1.838	1.934	1.966	1.982	1.991	1.998	2.002	2.005	2.024	2.027	2.027	2.028
z_2	3.987	4.503	4.663	4.735	4.775	4.800	4.818	4.831	4.897	4.907	4.910	4.911
z_3	5.651	6.647	7.256	7.532	7.664	7.737	7.853	7.854	7.951	7.968	7.973	7.975
z_4	7.738	8.412	9.023	9.677	10.18	10.487	10.655	10.753	11.045	11.070	11.078	11.080

Table 4: BIMATERIAL — Smallest positive solution $z_1, \ldots, z_4$ to (10).

The quantity $P_N(t)$ (resp. $\overline{P}_N(t)$) is the empirical mean number of particles moved with the real (resp. approximated) dynamic staying at the right side of the interface at time t, so that $P_N(t) \approx p_+(t)$.

With the spectral decomposition (12),

$$p_+(t) = \int_{L/2}^{L} \mathfrak{q}(t,x,y)\,\mathrm{d}y = \frac{1}{2} + \sum_{k=1}^{+\infty} c_k(x) e^{-\lambda_k^2 t} \tag{24}$$

where, for $\phi_k(\cdot)$ given by (11),

$$c_k(x) = \phi_k(x) \int_{L/2}^{L} \phi_k(y)\,\mathrm{d}y = \phi_k(x) \frac{\gamma_k}{\kappa_k \alpha_k^+} \sin\left(\alpha_k^+ \frac{L}{2}\right).$$

The first eigenvalue if $z_0 = 0$ corresponding to $\lambda_0^2 = 0$ and $\phi_0 = 1/\sqrt{L}$. We report on Table 4 for various ratios of $\rho = D^-/D^+$ the smallest positive solutions z_k to (10) with $0 < z_1 \leq z_2 \leq \cdots$. The eigenvalues $-\lambda_k^2$ are then easily obtained.

The steady-state (or stationary) regime is reached when $\mathfrak{q}(t,x,y)$ is close to a constant function and then when $c_1(x)\exp(-\lambda_1^2 t)$ is close to 0.

Thanks to the exponential term, a truncated version of the sum up to order 4 provides a good approximation of $p_+(t)$.

For each time t, $NP_N(t)$ is a binomial random variable with N trials and a probability of success $p_+(t)$. Using the normal approximation, $\sqrt{N}(P_N(t) - p_+(t))$ is close to a normal distribution $\mathcal{N}(0, p_+(t)(1-p_+(t)))$.

BIMATERIAL.. For a level of confidence α close to 1, check that for $t \in [0,T]$,

$$\sqrt{N}(\overline{P}_N(t) - p_+(t)) \in [-d_\alpha \sqrt{p_+(t)(1-p_+(t))}, d_\alpha \sqrt{p_+(t)(1-p_+(t))}]$$

with d_α given by (18).

For t large enough, $p_+(t)$ is close to $1/2$, and $P_N(t)$ fluctuates around $1/2$ with variance $1/4N$.

4.2.3 BIMATERIAL: Numerical results

We use the parameters given in Table 3.

The evolution of the positive probability $p_+(t)$ and its estimation is shown Figure 6 for $\rho = 20$. We see that all the schemes respect the global behavior of the $p_+(t)$ and fluctuates when the steady state regime is reached. However, for `SBMlin`, $\overline{P_N}(t)$ fluctuates around a value which is smaller than $1/2$, which means an incorrect repartition of the particles.

For each of the ratios, we plot in Figure 7 the normalized difference $t \mapsto \sqrt{N}(\overline{P_N}(t) - p_+(t))$ as well as the 99 %-confidence band. Unlike with `SBMlin`, the fluctuations of $\sqrt{N}(\overline{P_N}(t) - p_+(t))$ lies in the confidence interval for each t, which means that no bias could be distinguished from the Monte Carlo error for `SBM`, `Uffink` and `Hoteit`. For `SBMlin`, the fluctuations are in the right order, but there are in average more particles in the left-hand side of the media, where the diffusivity is higher. However, the mean of $\overline{P}_N(t)$ is of order $0.5 - 10^{-3}$, which is not an important error. This is due to the phenomena observed in Figure 3 for the LAYER test close to the interface. The SYMMETRY benchmark test also gives some insight about this (See Section 4.4.1).

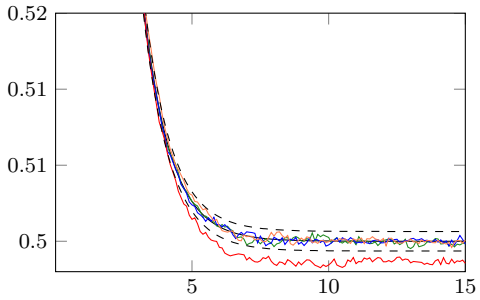

Figure 6: BIMATERIAL — Plots of $t \mapsto p_+(t)$ (black), 99 %-confidence band $t \mapsto p_+(t) \pm N^{-1/2} d_{0.99} \sqrt{p_+(t)(1-p_+(t))}$ (dashed) and $t \mapsto \overline{P}_N(t)$ for $\rho = 20$ and the four methods: `SBM`, `Uffink`, `Hoteit` and `SBMlin`.

Although there is no benchmark test attached to it, we show in Figure 8 the evolution of number of particles which cross the interface from the right part to the left part during a time step δt. This quantity represents δt times the flow of particles from the right to the left. We have checked that the same amount of particles go from the right to the left and from the left to the right once the steady state regime is reached. However the flow of particles for `Hoteit` and `SBMlin` is around half of the flow of particles for `SBM` and `Uffink`. Since `SBM` is an exact method, `Uffink` slightly overestimates the flow of particles, while `Hoteit` and `SBMlin` underestimate this quantity. This could explain why for these two

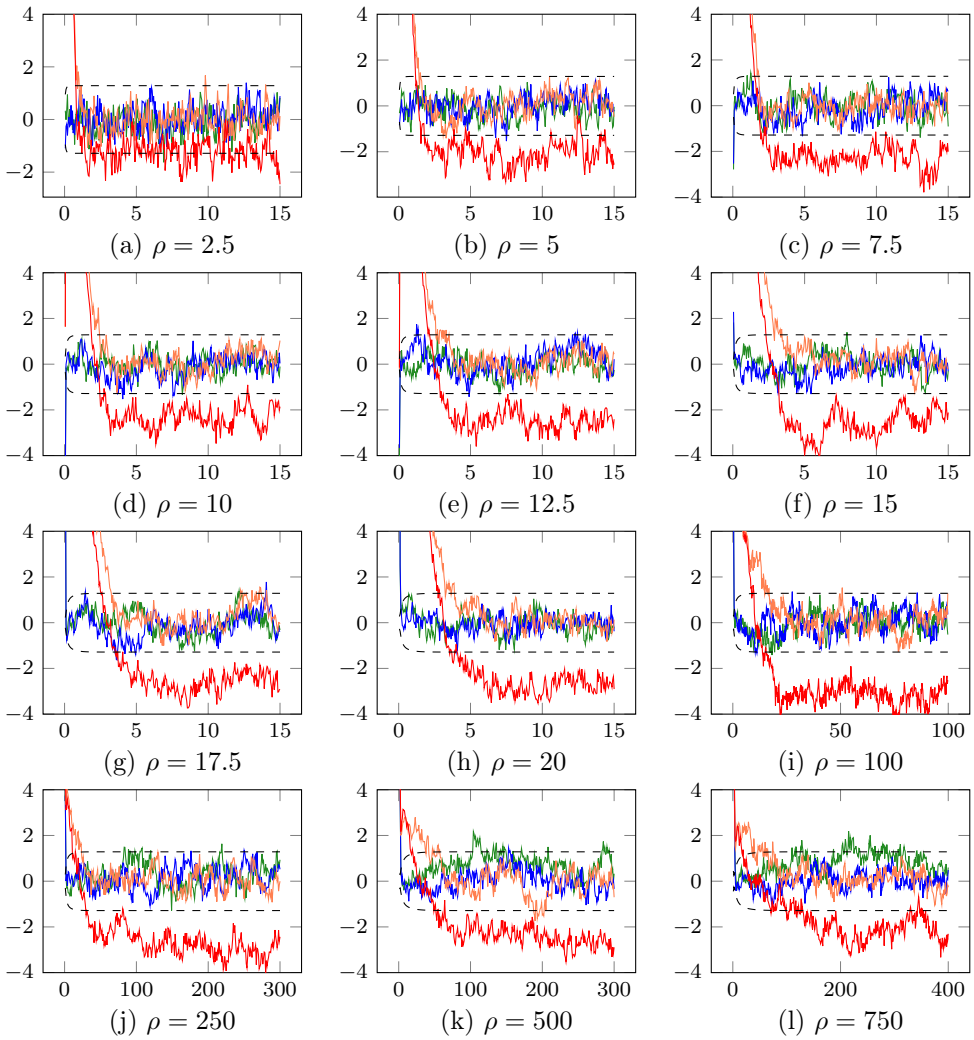

Figure 7: BIMATERIAL — Plot of $t \mapsto \sqrt{N}(P_N(t) - p_+(t))$ for the four methods: SBM, Uffink, Hoteit and SBMlin and comparison with the 99 %-confidence band $t \mapsto \pm d_{0.99}\sqrt{p_+(t)(1-p_+(t))}$.

methods, $\overline{P}_N(t)$ differs significantly from $p_+(t)$ in the transient regime. However, for large values of ρ, all the values tend to converge quickly towards a very small probability of passage.

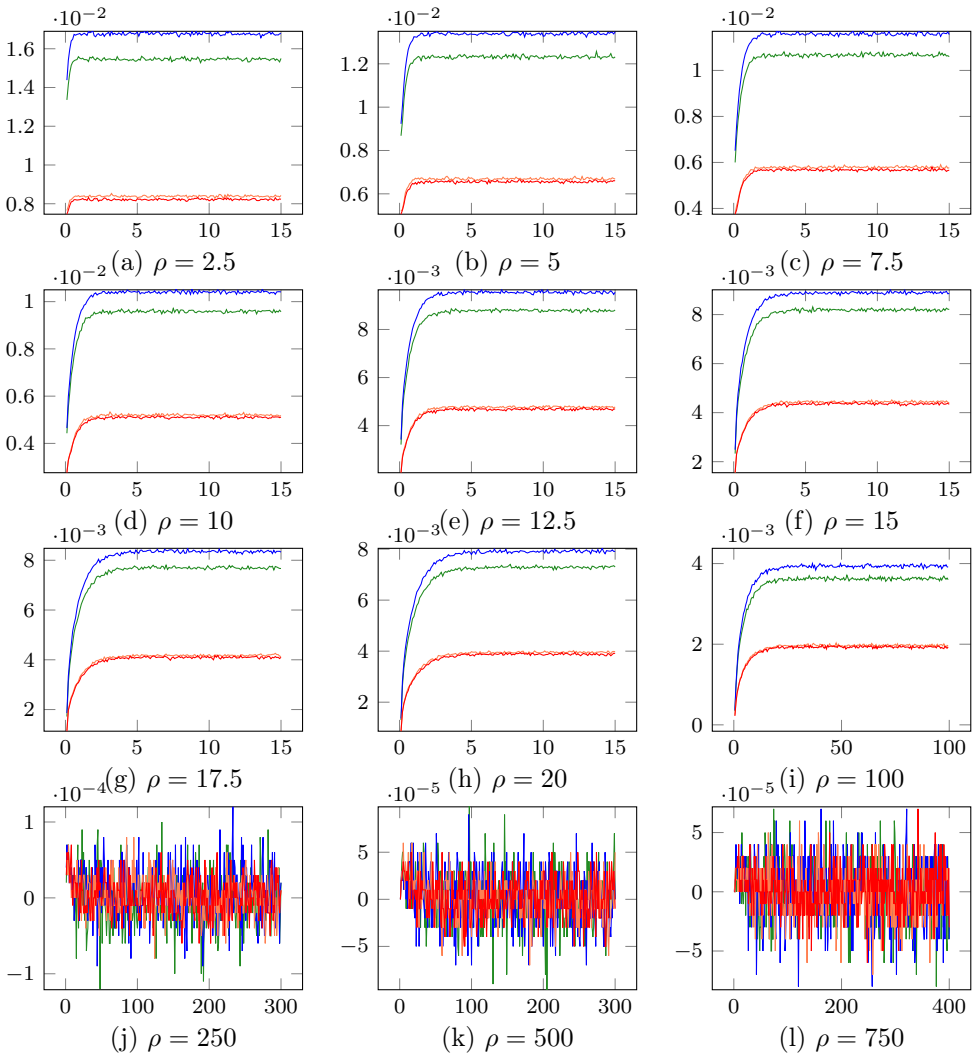

Figure 8: BIMATERIAL — Empirical estimation of the mean number of particles going from the right part to the left part between t and $t + \delta t$ in function of t for the four methods SBM, Uffink, Hoteit and SBMlin.

4.3 BIMATERIAL ABSORBING benchmark test: check if the first exit time is correctly estimated

4.3.1 BIMATERIAL ABSORBING: Description

An absorbing BC condition at L means that the particles are removed from the medium when reaching L, leading to a loss of mass. Let X be the stochastic process associated to $\nabla(D\nabla\cdot)$ in a medium with an absorbing BC. The *first exit time* is the random variable τ which gives the first time at which the particle

ρ	2.5	5	7.5	10	12.5	15	17.5	20	100	250	500	750
$\widetilde{z}_0$	0.830	0.845	0.850	0.853	0.854	0.855	0.856	0.856	0.860	0.860	0.860	0.860
$\widetilde{z}_1$	2.951	3.204	3.283	3.321	3.343	3.357	3.368	3.375	3.416	3.422	3.424	3.424
$\widetilde{z}_2$	4.840	5.698	6.024	6.159	6.229	6.271	6.299	6.319	6.416	6.429	6.433	6.435
$\widetilde{z}_3$	6.630	7.449	8.221	8.748	9.024	9.167	9.249	9.301	9.496	9.517	9.523	9.525
$\widetilde{z}_4$	8.799	9.617	10.002	10.487	11.051	11.551	11.902	12.115	12.599	12.628	12.637	12.640

Table 5: BIMATERIAL ABSORBING — Smallest positive solutions $\widetilde{z}_0, \ldots, \widetilde{z}_4$ to (15) in function of $\rho = D^-/D^+$.

hits an absorbing BC. The distribution function $G(t) = 1 - \mathbb{P}[\tau > t]$ of τ is the proportion of particles remaining in the medium at time t. This function $G(t)$ is related to *breakthrough curves* [59] and *mean residence time* [6].

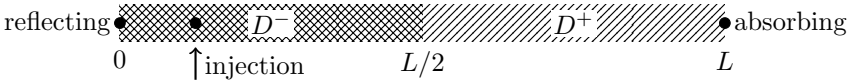

Figure 9: Medium for the BIMATERIAL ABSORBING test.

In Section 2.5, we gave an explicit formula for the distribution function G, for a medium of Figure 9, to which we compare its empirical approximation $\overline{G}_N$ when one of the schemes is used.

4.3.2 BIMATERIAL ABSORBING I: Benchmark test definition

For the particles starting from x, with (13) and (14),

$$G(t) = \mathbb{P}[\tau \le t] = \sum_{k=0}^{+\infty} e^{-\widetilde{\lambda}_k^2 t} \widetilde{\phi}_k(x) \int_0^L \widetilde{\phi}_k(y)\,\mathrm{d}y$$

with $\widetilde{\phi}_k$ given by (16) and

$$\int_0^L \widetilde{\phi}_k(y)\,\mathrm{d}y = \frac{\sin(\widetilde{\alpha}^- L/2)}{\widetilde{\alpha}^- \widetilde{\kappa}_k} - \widetilde{\gamma}_k \frac{\cos(\widetilde{\alpha}^+ L/2)}{\widetilde{\alpha}^+ \widetilde{\kappa}_k} + \frac{\widetilde{\gamma}_k}{\widetilde{\alpha}^+ \widetilde{\kappa}_k}.$$

The values of the smallest positive roots $\widetilde{z}_0, \ldots, \widetilde{z}_4$ of (15) are given in Table 5.

We simulate for N particles the first time τ at which they reach the boundary where an absorbing BC holds.

Let $\overline{G}_N$ be the empirical distribution function of the first exit time τ with one of the schemes is used (See the entry *boundary layer* in Table 2 for the algorithm used to compute the exit time).

BIMATERIAL ABSORBING I. For a confidence level α, check if $\sqrt{N}(\overline{G}_N(t) - G(t))$ belongs to the confidence band $t \mapsto \pm d_\alpha \sqrt{G(t)(1-G(t))}$.

4.3.3 Bimaterial absorbing I: Numerical results

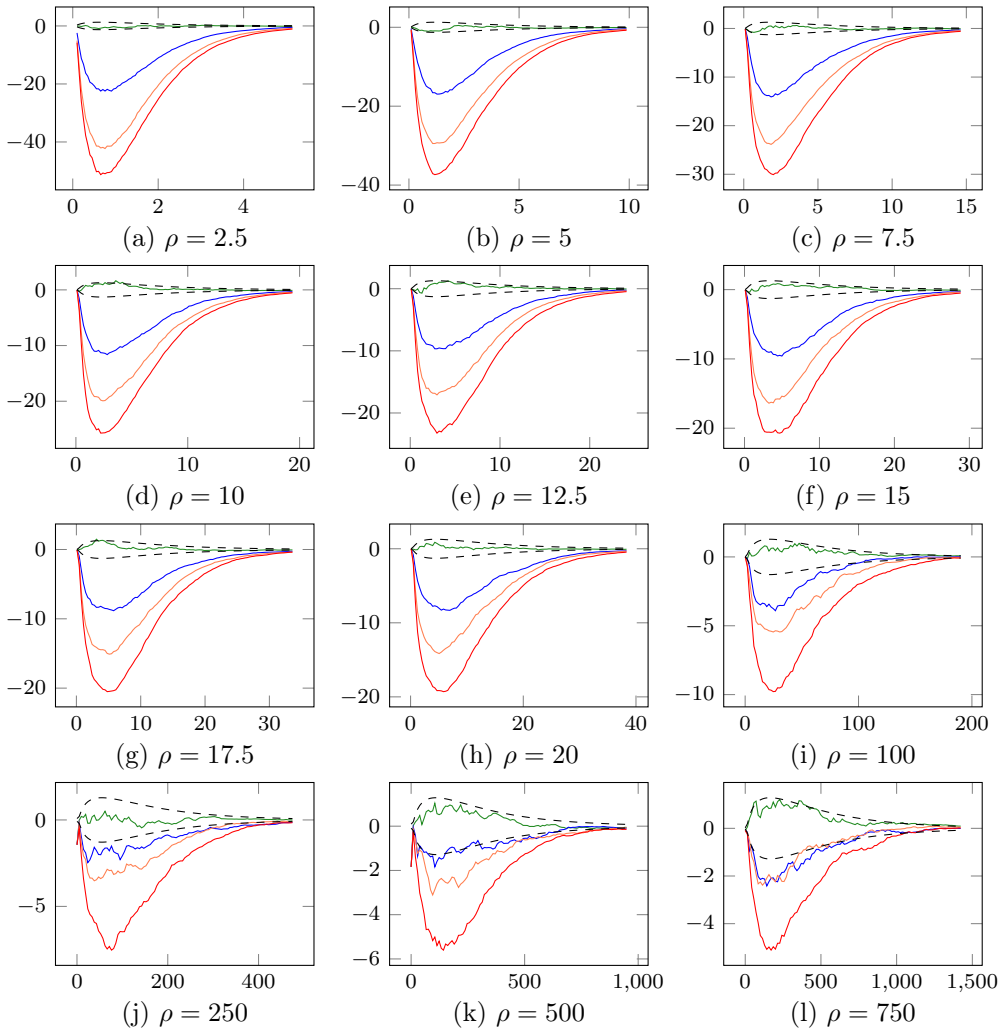

Figure 10: Bimaterial absorbing I — Plots of $\sqrt{N}(G_N(t) - G(t))$ for the true distribution function G of the exit time τ and the empirical distribution function of the exit time using the schemes `SBM+ExactHittingTime`, `Uffink+LinearHittingTimeUS`, `Hoteit+LinearHittingTimeUS` and `SBMlin+LinearHittingTimeGS`. The dashed lines represents the 99 % confidence band $t \mapsto \pm d_{0.99}\sqrt{G(t)(1-G(t))}$.

We plot in Figure 10 the difference between the true and the empirical distribution functions of τ.

Excepted for `SBM+ExactHittingTime` , the difference $\sqrt{N}(G_N(t) - G(t))$ is too important to come from the Monte Carlo error. This is not surprising. From their

very construction, the `LinearHittingTimeUS` and `LinearHittingTimeGS` methods overestimate the first exit time τ. Indeed, with these methods, the first guess is accepted as a new position if it remains in the domain. This neglects the event that the particle may leave the domain during the time step. Nevertheless, since `Uffink` and `Hoteit` are combined with the same method `LinearHittingTimeUS`, this benchmark test demonstrates that the schemes at the interface have really an influence of the whole quality of the breakthrough curve and that `Uffink` performs better than `Hoteit`. Better schemes than `LinearHittingTimeUS` may be sought for dealing with the exit time. However, caution must be observed when designing such schemes as mixing schemes in the different zones may introduce additional errors as illustrated in Section 5.2. The way we combined the algorithms in Table 2 follows this recommendation.

Let us note also that the deviation of $\overline{G}_N$ from G is less important for large ratios.

4.3.4 Bimaterial absorbing II: Benchmark test definition

It follows from the Bimaterial absorbing I benchmark tests that `SBM` is recommended for a fine estimate of the breakthrough curve. However, some applications requires only an accurate estimation of the rate of convergence towards 0 of the survival probability $1 - G(t)$. We propose a second benchmark test which relies on estimating this rate of convergence.

With (17) (See Figure 11),

$$\log(1 - G_N(t)) \approx \log(\widetilde{\kappa}) - \widetilde{\lambda}_0^2 t.$$

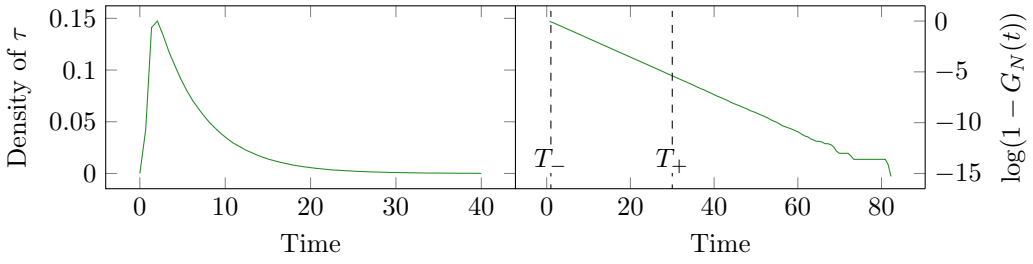

Figure 11: Bimaterial absorbing II — Estimation of the exponential convergence of $1 - \overline{G}_N(t)$ to 0.

We use as in [36] a linear least squares on $t \mapsto \log(1-\overline{G}_N(t))$ on a window $[T_-, T_+]$. The choice of T_- and T_+ is crucial. On the one hand, T_- should be chosen large enough to avoid that $\exp(-\widetilde{\lambda}_0^2 t)$ dominates all the other terms. On the other hand, due to a rare event estimation problem, $\log(1-\overline{G}_N(t))$ tends to oscillate for t large

enough. This means that the Monte Carlo error, of order $\sqrt{\overline{G}_N(t)(1-\overline{G}_N(t))/N}$ is much more bigger than $1-G(t)$. Thus, T_+ shall be chosen small enough to avoid the oscillations of $\log(1-\overline{G}_N(t))$ (See Figure 11).

Bimaterial absorbing II. Estimate $\widetilde{\lambda}_0^2$ from a linear least squares procedure on $t \in [T_-, T_+] \mapsto \log(1-\overline{G}_N(t))$, where $\overline{G}_N$ is the empirical distribution function of the first exit time from the domain by the absorbing boundary using one of the scheme.

4.3.5 Bimaterial absorbing II: Numerical results

For each method and our choice of ratios, $t \mapsto \log(1-\overline{G}_N(t))$ is plotted in Figure 12, and relative errors of the estimation of $-\widetilde{\lambda}_0^2$ are given.

`SBM+ExactHittingTime` performs the best and provides us with an accurate estimation of the exponential rate. The other combinations methods underestimate this quantity, especially for small ratio. However, the results are rather good for all the methods for a qualitative description of the rate of loss of mass. At large ratio, it is more difficult to differentiate between the different methods. This phenomena was already observed in Bimaterial absorbing I.

4.4 Symmetry benchmark tests: check if the density transition function of the scheme is symmetric

With periodic or reflecting BC at the endpoints 0 and L, the operator $\nabla(D\nabla\cdot)$ is self-adjoint and then $\mathfrak{q}(t,x,y) = \mathfrak{q}(t,x,y)$ for any $(x,y) \in [0,L]^2$. This means that the probability to go from x into a small volume $\mathrm{d}\mathcal{V}$ around y is the same as the probability to go from y into a small volume $\mathrm{d}\mathcal{V}$ around x. This property implies immediately that the Lebesgue measure is invariant measure for the dynamic.

4.4.1 Symmetry: Description

We use a bimaterial medium as in Figure 5 and we denote by p_{-+} (resp. p_{+-}) the proportion of particles during $[0,t]$ that goes from the compartment at the left ($x \le L/2$) (resp. right) to the compartment at the right ($x \ge L/2$) (resp. left) of the discontinuity. If the particles are uniformly distributed on each compartment, then

$$p_{-+} = \frac{2}{L}\int_0^{L/2} \mathrm{d}x \int_{L/2}^{L} \mathrm{d}y\, \mathfrak{q}(t,x,y) = \frac{2}{L}\int_{L/2}^{L} \mathrm{d}x \int_0^{L/2} \mathrm{d}y\, \mathfrak{q}(t,x,y) = p_{+-}.$$

The symmetry property of $\mathfrak{q}(t,x,y)$ guarantees the correct exchange of particles between each compartment and the global equilibrium.

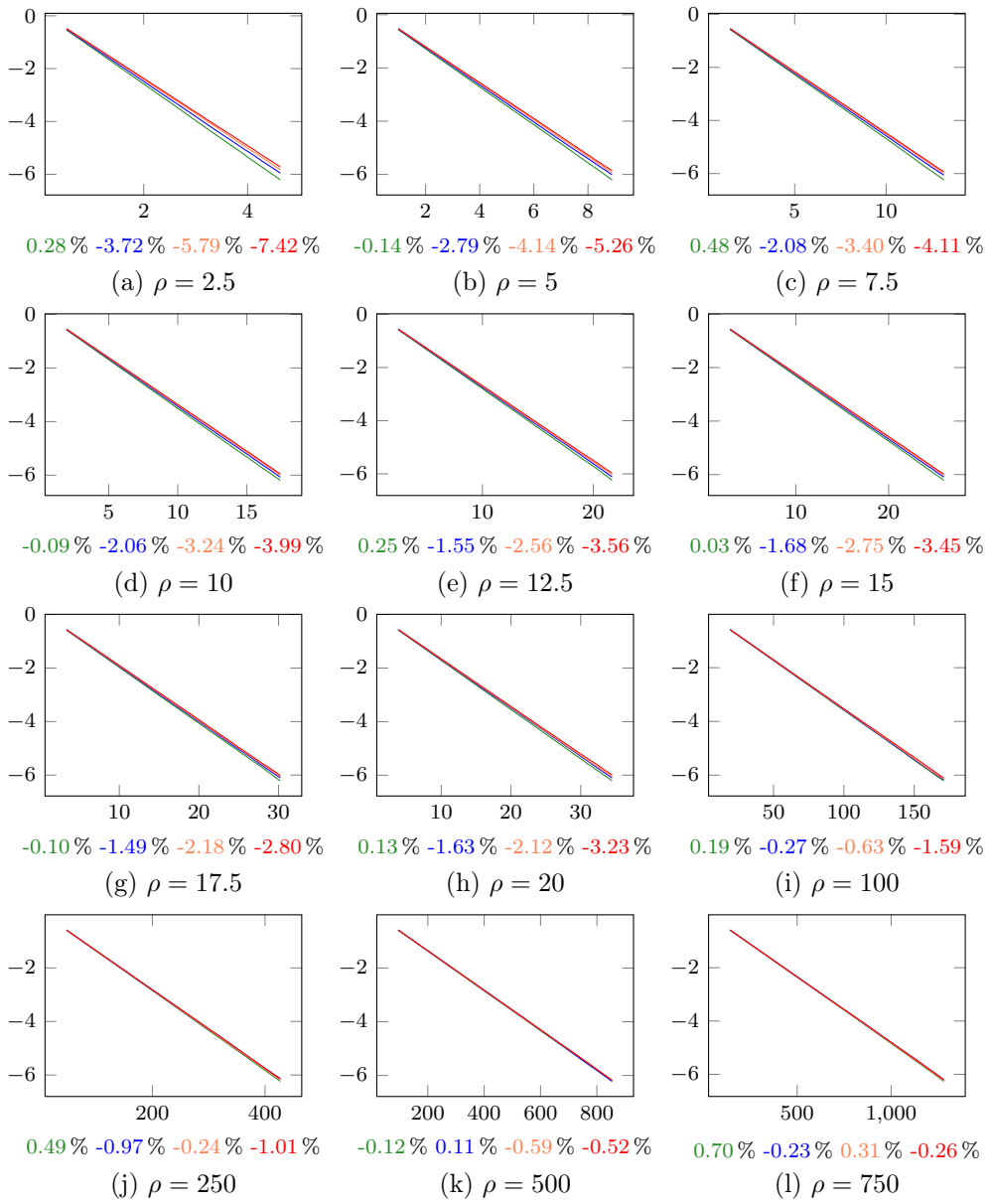

Figure 12: BIMATERIAL ABSORBING II — Plot of $t \mapsto \log(1 - \overline{G}_N(t))$ for $t \in [T/10, 9T/10]$. The relative error $100 \times (\lambda_0^2 - a)/\lambda_0^2$, where a is the slope of $t \in [T/10, 9T/10] \mapsto \log(1 - \overline{G}_N(t))$ estimated by a least squares procedure, is reported at the bottom of each graph for each of the methods `SBM+ExactHittingTime`, `Uffink+LinearHittingTimeUS`, `Hoteit+LinearHittingTimeUS` and `SBMlin+LinearHittingTimeGS` using the color code of Table 1.

4.4.2 SYMMETRY: Benchmark test definition

The domain $[0, L]$ is cut into small intervals $[iL/n, (i+1)L/n]$, $i = 0, \dots, n-1$. For N particles $X^{(1)}, \dots, X^{(N)}$, set

$$Q_{ij}(t) = \frac{L}{n} \frac{\#\{k \text{ such that } X_t^{(k)} \in [jL/n, (j+1)L/n] \text{ when } X_0 = x_i\}}{N} \approx \int_{jL/n}^{(j+1)L/n} \overline{\mathfrak{q}}(t, (i+1/2)L/n, y)\, \mathrm{d}y.$$

SYMMETRY. Plot the difference $\Delta_{ij}(t) = |Q_{ij}(t) - Q_{ji}(t)|$ as function of $i, j = 0, \dots, n-1$.

The quantity $\Delta_{ij}(t)$ measures of how much numerically the density $\overline{\mathfrak{q}}(t, x, y)$ of the scheme deviates from being symmetric in x and y.

Here, we do not quantify the statistical fluctuations of $Q_{ij}(t)$, but it appears in our numerical results that it is not crucial as for the other benchmark tests.

4.4.3 SYMMETRY: Numerical results

The discrete density $Q_{i,j}(T)$ and the symmetric difference $\Delta_{i,j}(T)$ for the four scheme are plotted as function of (i, j) in Figures 13 and 14 at times $T = 0.01$ and $T = 0.2$. We used the parameters given in Table 3.

The symmetry is well preserved by the exact scheme `SBM`, and after several time steps, by `Uffink`. This is not the case for the other schemes. At $T = 0.01$, the maximum of $(\Delta_{i,j}(T))_{i,j=0,\dots,n-1}$ is 0.05 for `SBM`, 0.29 for `Hoteit`, 0.52 for `Uffink` and 0.21 for `SBMlin`. However, for this last scheme, there are more points at which $(\Delta_{i,j}(T))_{i,j=0,\dots,n-1}$ is high. In addition, the higher values of $(\Delta_{i,j})_{i,j=0,\dots,n-1}$ "propagates" as the time evolves. This could explain the bad performance of `SBMlin` in regard to the other schemes for our benchmark tests BIMATERIAL and LAYER.

5 Caution

Some examples show that one has to carefully choose the size of the medium as well as the combination of the algorithms in order to get relevant benchmarks.

5.1 Size of the domain

We plot in Figure 15 the distribution of 2×10^6 particles in the steady state regime with `SBMlin`. What is plotted is really an empirical estimation of the density of X_t

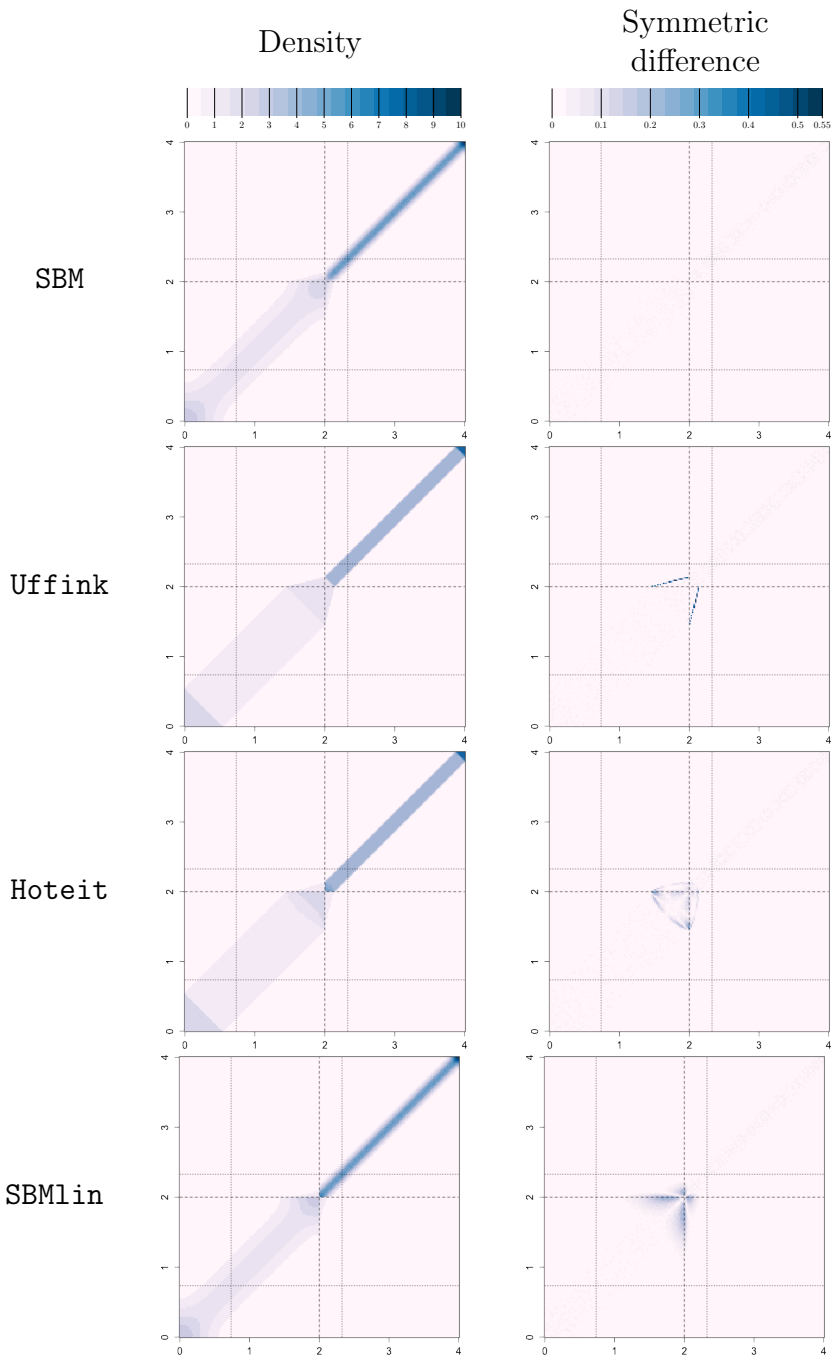

Figure 13: SYMMETRY — Discrete density $(Q_{i,j}(\delta t))_{i,j=0,\dots,n-1}$ and $(\Delta_{i,j}(\delta t))_{i,j=0,\dots,m-1}$ after one time step $\delta t = 0.01$ in a bimaterial medium with $D^- = 5$ and $D^+ = 1/3$, an interface at $x_I = 2$ and reflecting boundary conditions at $x = 0$ and $x = 4$.

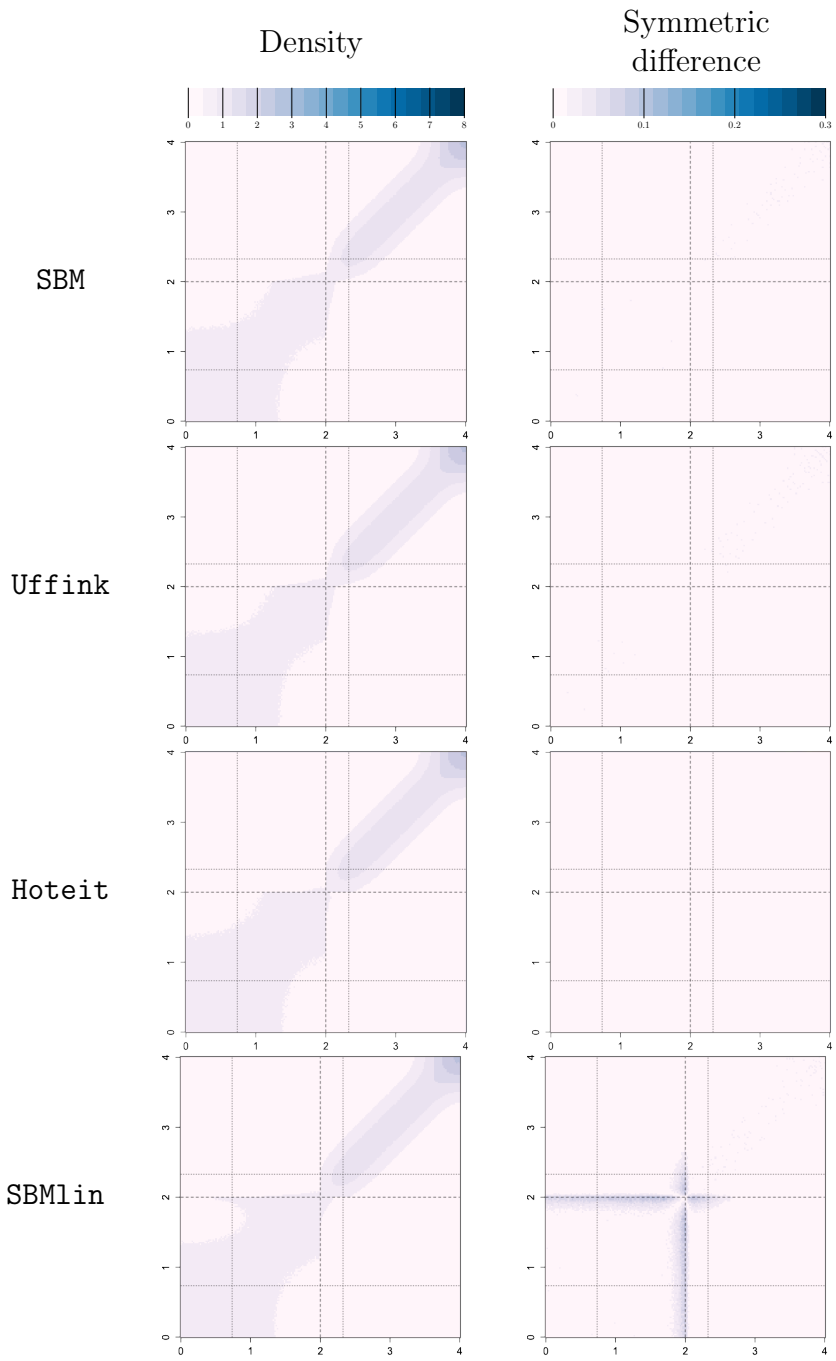

Figure 14: SYMMETRY — Discrete density $(Q_{i,j}(T))_{i,j=0,\dots,m-1}$ and $(\Delta_{i,j}(T))_{i,j=0,\dots,m-1}$ at time $T = 0.2$, with $\delta t = 0.01$, in a bimaterial medium with $D^- = 5$ and $D^+ = 1/3$, an interface at $x_I = 2$ and reflecting boundary conditions at $x = 0$ and $x = 4$.

at time $T = 10$ ($\delta t = 0.001$), with an initial uniform distribution in a bimaterial medium with $D^- = 5$ and $D^-/D^+ = \rho$ and reflecting BC. In Figure 15(a), for a domain size of 2, the bias of the scheme is visible around the interface. In Figure 15(b), for a domain size of 50, the bias of the scheme is small in front of the statistical fluctuations, as it only affect a relatively small quantity of particles.

This is why we have chosen interface layers that are as big as possible with respect to the total size of the medium.

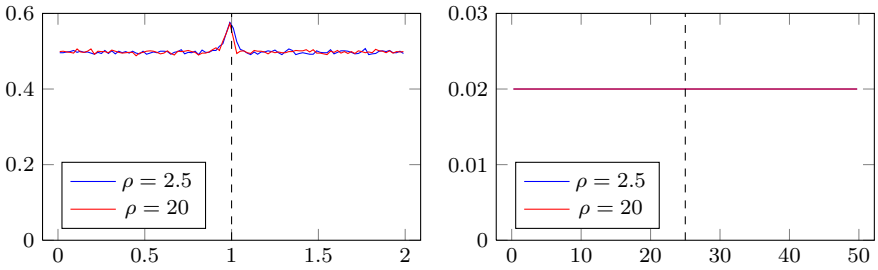

(a) Size of the media: 2 (b) Size of the media: 50

Figure 15: Influence of the size of the domain: empirical estimation of the density of X_t. Example with a bimaterial medium in the steady state regime and `SBMlin` at time $T = 10$.

5.2 Mixing the schemes

Table 2 of Section 3 describes the way we have coupled the schemes in the different zones. Other choices could have been performed. However, this leads to bad results.

In Figure 16, we show the effect of mixing the `Hoteit` scheme in the interface layer with the `GaussianStep` outside the interface layer in a bimaterial medium. With a uniform repartition of the particles and reflected boundary conditions at 0 and 2, the particle shall remain uniformly distributed all over the medium. This is not the case around the limits of the interface layers. Similar results occurs with other ways of mixing the schemes.

Since `Uffink` and `Hoteit` rely on uniform approximation, they should be coupled with schemes relying on uniform approximations to avoid bad behavior when the particle is moved from one zone to another.

6 Conclusion

We have studied four Monte Carlo simulation techniques giving rules to move particles close the interface between two media with different diffusivities.

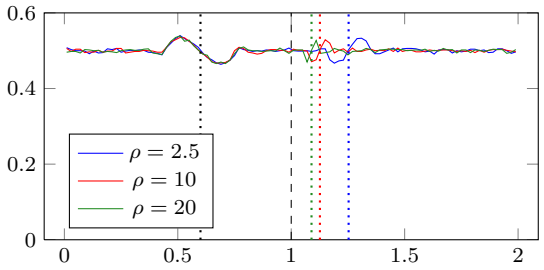

Figure 16: Histograms of the positions of 2×10^6 particles at time $T = 10$ ($\delta t = 0.001$) in a bimaterial medium with reflected BC for `Hoteit` coupled with `GaussianStep` outside the interface layer. The dotted lines represent the limits of the interface layers for three values of ρ, while the dashed line represents the interface.

We have also set us simple benchmark tests which are physically and numerically relevant and backed by a statistical methodology to discriminate between the possible bias and the Monte Carlo error.

We have considered simple media, but our methodology extends well to media with multiples layers. We plan to perform further tests in more realistic media using the software `PARADIS` (PARAllel DISpersion) [4, 13].

Note however that these benchmark tests have to be properly redefined in presence of a convective term, where the infinitesimal generator of X is self-adjoint, but not with respect to the Lebesgue measure. In this case, the benchmark tests need to be adapted.

According to the numerical results, `SBM` is successful for all benchmark tests: it provide a correct repartition of the particles, as well as a correct rate of convergence towards the steady state regime and it preserves the symmetry of the density, even after many steps.

With `Uffink` and `Hoteit` schemes, although the particles are not replaced accurately close to the interface, the repartition of particles and the rate of convergence towards the steady state regime are correct, the symmetry property is rather well respected. However they do not perform as good as `SBM+ExactHittingTime` in the BIMATERIAL ABSORBING test mainly because they are combined with `LinearHittingTimeUS` which overestimate the first exit time from the medium. Nevertheless, this benchmark shows that `Uffink` provides better results than `Hoteit`. Moreover, in the BIMATERIAL TEST, it is shown that `Uffink` respects well the flow of particles.

With `SBMlin`, even if it uses the same way to compute the passage time through the interface as `Hoteit`, it breaks the symmetry of the density, even after many steps.

In the BIMATERIAL test, the proportion of particles on each side of the interface is not well respected. In the BIMATERIAL ABSORBING test, it also overestimates the first exit time from the medium.

Hence, the methods `SBM`, `Uffink` and `Hoteit` are globally valid in all the situation despite they do not behave the same in all the situations. We then recommend the use of `SBM` if possible and if this scheme is compatible with the way the particles are moved away from the interface. Otherwise, we recommend, especially in the transient regime, `Uffink` and then `Hoteit`. With absorbing BC, we recommend to look for a better scheme than the simple `LinearHittingTimeUS` to estimate the first exit time. The scheme `SBMlin` fails the tests and should be then avoided.

Thus, we provide a guide for choosing between the different schemes. For applications for which the information at the macroscopic scales is sufficient, a scheme that respects some qualitative behaviors (mean residence time, ...) could be chosen, as `Uffink`, `Hoteit` or `SBM`. However, for some other applications, it can be important to quantify finer behaviors (mass flow, positions of particles close to the interface, breakthrough curve, ...) as for example, when the particles are associated to chemical species that react with the media or interact with each other. In these cases, accurate scheme like `SBM` should be chosen.

Acknowledgments. This work was supported by ANR-MN, with the H2MNO4 project. Computer simulations related to this work were performed on the ADA cluster at the Institut du Développement et des Ressources en Informatique Scientifique (IDRIS), Orsay, France.

Bibliography

[1] P. Ackerer and R. Mose, *Comment on "Diffusion theory for transport in porous media: Transition-probability densities of diffusion processes corresponding to advection-dispersion equations" by Eric M. LaBolle et al.*, Water Resour. Res. **36** (2000), no. 3, 819–821.

[2] T.A. Appuhamillage, V.A. Bokil, E. Thomann, E. Waymire, and B. D. Wood, *Solute transport across an interface: A Fickian theory for skewness in breakthrough curves*, Water Resour. Res., **46** (2010), W07511, DOI 10.1029/2009WR008258.

[3] _____, *Occupation and local times for Skew Brownian motion with application to dispersion accross an interface*, Ann. Appl. Probab. **21** (2011), no. 1, 183–214, DOI 10.1214/10-AAP691.

[4] A. Beaudoin, J.R. de Dreuzy, J. Erhel, and G. Pichot, *Convergence analysis of macro spreading in 3D heterogeneous porous media*, ESAIM: Proceedings (2013).

[5] M. Bechtold, J. Vanderborght, O. Ippisch, and H.V. Vereecken, *Efficient random walk particle tracking algorithm for advective-dispersive transport in media with discontinuous dispersion coefficients and water contents*, Water Resour. Res., **47** (2011), W10526.

[6] A.M. Berezhkovskii, V. Zaloj, and N. Agmon, *Residence time distribution of a Brownian particle*, Physical Review E **57** (1998), no. 4, 3937–3947.

[7] M. Bossy, N. Champagnat, S. Maire, and D. Talay, *Probabilistic interpretation and random walk on spheres algorithms for the Poisson-Boltzmann equation in Molecular Dynamics*, ESAIM M2AN **44** (2010), no. 5, 997–1048.

[8] R.S. Cantrell and C. Cosner, *Diffusion Models for Population Dynamics Incorporating Individual Behavior at Boundaries: Applications to Refuge Design*, Theor. Popul. Biol. **55** (1999), no. 2, 189–207, DOI 10.1006/tpbi.1998.1397.

[9] A. Cortis and A. Zoia, *Model of dispersive transport across sharp interfaces between porous materials*, Phys. Rev. E **80** (2009), 011122.

[10] D. R. Cox and D. V. Hinkley, *Theoretical statistics*, Chapman and Hall, London, 1974.

[11] J.-R. de Dreuzy, G. Pichot, B. Poirriez, and J. Erhel, *Synthetic benchmark for modeling flow in 3D fractured media*, Computers & Geosciences **50** (2013), 59-71, DOI 10.1016/j.cageo.2012.07.025.

[12] F. Delay, Ph. Ackerer, and C. Danquigny, *Simulating Solute Transport in Porous or Fractured Formations Using Random Walks Particle Tracking: A Review*, Vadose Zone J. **4** (2005), 360–379.

[13] J. Erhel and J.-R. de Dreuzy and A. Beaudoin and E. Bresciani and D. Tromeur-Dervout, *A parallel scientific software for heterogeneous hydrogeology*, Parallel Computational Fluid Dynamics 2007, 2009, pp. 39-48. Invited plenary talk.

[14] P. Étoré, *On random walk simulation of one-dimensional diffusion processes with discontinuous coefficients*, Electron. J. Probab. **11** (2006), no. 9, 249–275.

[15] P. Étoré and A. Lejay, *A Donsker theorem to simulate one-dimensional processes with measurable coefficients*, ESAIM Probab. Stat. **11** (2007), 301–326, DOI 10.1051/ps:2007021.

[16] P. Étoré and M. Martinez, *Exact simulation of one-dimensional stochastic differential equations involving the local time at zero of the unknown process*, Monte Carlo Methods Appl. **19** (2013), no. 1, DOI 10.1515/mcma-2013-0002.

[17] W. Feller, *On the Kolmogorov-Smirnov limit theorems for empirical distributions*, Ann. Math. Statistics **19** (1948), 177–189.

[18] E. Fieremans, D. S Novikov, J. H. Jensen, and J. A. Helpern, *Monte Carlo study of a two-compartment exchange model of diffusion*, NMR Biomed. **23** (2010), 711–724, DOI 10.1002/nbm.1577.

[19] M. Fisz, *Probability theory and mathematical statistics*, John Wiley & Sons Inc., New York, 1963.

[20] C. Gardiner, *Stochastic methods. A handbook for the natural and social sciences*, 4th ed., Springer Series in Synergetics, Springer-Verlag, Berlin, 2009.

[21] U. Gräwe, E. Deleersnijder, S. H. A. M. Shah, and A. W. Heemink, *Why the Euler scheme in particle tracking is not enough: the shallow-sea pycnocline test case*, Ocean Dynamics **62** (2012), no. 4, 501–514.

[22] U. Gräwe, *Implementation of high-order particle-tracking schemes in a water column model*, Ocean Modelling **36**, no. 1-2, 80–89, DOI 10.1016/j.ocemod.2010.10.002.

[23] H.W. de Haan, M. Chubynsky, and G.W. Slater, *Monte Carlo Approaches for Simulating a Particle at a Diffusivity Interface and the "Ito–Stratonovich Dilemma"* (August 24, 2012), available at `arxiv:1208.5081v1`.

[24] R. Herbin and F. Hubert, *Benchmark on Discretization Schemes for Anisotropic Diffusion Problems on General Grids*, Proceedings of Finite Volumes for Complex Applications V (Aussois, France), Hermès, 2008.

[25] H. Hoteit, R. Mose, A. Younes, F. Lehmann, and Ph. Ackerer, *Three-dimensional modeling of mass transfer in porous media using the mixed hybrid finite elements and the random-walk methods*, Math. Geology **34** (2002), no. 4, 435–456.

[26] P. E. Kloeden and E. Platen, *Numerical solution of stochastic differential equations*, Applications of Mathematics (New York), vol. 23, Springer-Verlag, Berlin, 1992.

[27] O. Kolditz and H. Shao (eds.), *OpenGeoSys Developer-Benchmark-Book (OGS-DBB 5.04)*, UFZ Publisher, August 2010.

[28] N.H. Kuiper, *Tests concerning random points on a circle*, Proc. Koninkl. Nederl. Akad. Van Wettenschappen, Series A **63** (1960), 38–47.

[29] E. M. LaBolle and Y. Zhang, *Reply to comment by D.-H. Lim on "Diffusion processes in composite porous media and their numerical integration by random walks: Generalized stochastic differential equations with discontinuous coefficients"*, Water Resour. Res. **42** (2006), W02602, DOI 10.1029/2005WR004403.

[30] E. M. LaBolle, J. Quastel, G. E. Fogg, and J. Gravner, *Diffusion processes in composite porous media and their numerical integration by random walks: Generalized stochastic differential equations with discontinuous coefficients*, Water Resour. Res. **36** (2000), 651–662, DOI 10.1029/1999WR900224.

[31] E. M. LaBolle, G.E. Fogg, and A.F.B. Thomson, *Random-Walk Simulation of Transport in Heterogeneous Porous Media: Local Mass-Conservation Problem and Implementation Methods*, Water Resour. Res., **32** (1996), no. 3, 582–593, DOI 10.1029/95WR03528.

[32] A. Lejay and G. Pichot, *Simulating diffusion processes in discontinuous media: a numerical scheme with constant time steps*, J. Comput. Phys. **231** (2012), no. 21, 7299–7314, DOI 10.1016/j.jcp.2012.07.011.

[33] A. Lejay, *On the constructions of the Skew Brownian motion*, Probab. Surv. **3** (2006), 413–466.

[34] A. Lejay and M. Martinez, *A scheme for simulating one-dimensional diffusion processes with discontinuous coefficients*, Ann. Appl. Probab. **16** (2006), no. 1, 107–139, DOI 10.1214/105051605000000656.

[35] A. Lejay, *Simulating a diffusion on a graph. Application to reservoir engineering*, Monte Carlo Methods Appl. **9** (2003), no. 3, 241–256.

[36] A. Lejay and S. Maire, *Computing the principal eigenvalue of the Laplace operator by a stochastic method*, Math. Comput. Simulation **73** (2007), no. 3, 351–363, DOI 10.1016/j.matcom.2006.06.011.

[37] D.-H. Lim, *Comment on "Diffusion processes in composite porous media and their numerical integration by random walks: Generalized stochastic differential equations with discontinuous coefficients" by E. M. LaBolle, J. Quastel, G. E. Fogg, and J. Gravner*, Water Resour. Res. **42** (2006), W02601, DOI 10.1029/2005WR004091.

[38] A. Marcowith and F. Casse, *Postshock turbulence and diffusive shock acceleration in young supernova remnants*, Astron. Astrophys. **515** (2010), no. A90, DOI 10.1051/0004-6361/200913022.

[39] M. Marseguerra and A. Zoia, *Normal and anomalous transport across an interface: Monte Carlo and analytical approach*, Ann. Nucl. Energy **33** (2006), no. 17–18, 1396–1407, DOI 10.1016/j.anucene.2006.09.012.

[40] M. Martinez, *Interprétations probabilistes d'opérateurs sous forme divergence et analyse de méthodes numériques associées*, PhD thesis, Université de Provence / INRIA Sophia-Antipolis, 2004.

[41] M. Martinez and D. Talay, *Discrétisation d'équations différentielles stochastiques unidimensionnelles à générateur sous forme divergence avec coefficient discontinu*, C. R. Math. Acad. Sci. Paris **342** (2006), no. 1, 51–56, DOI 10.1016/j.crma.2005.10.025.

[42] ———, *One-Dimensional parabolic diffraction equations: Pointwise estimates and discretization of related stochastic differential equations with weighted local times*, Electron. J. Probab. **17** (2012), no. 27, DOI 10.1214/EJP.v17-1905.

[43] M. Mascagni and N. A. Simonov, *Monte Carlo methods for calculating some physical properties of large molecules*, SIAM J. Sci. Comput. **26** (2004), no. 1, 339–357, DOI 10.1137/S1064827503422221.

[44] G. N. Milstein and M. V. Tretyakov, *Stochastic numerics for mathematical physics*, Scientific Computation, Springer-Verlag, Berlin, 2004.

[45] B. Øksendal, *Stochastic differential equations: An introduction with applications*, 6th ed., Universitext, Springer-Verlag, Berlin, 2003.

[46] O. Ovaskainen and S. J. Cornell, *Biased movement at a boundary and conditional occupancy times for diffusion processes*, J. Appl. Probab. **40** (2003), no. 3, 557–580.

[47] J. M. Ramirez, E. A. Thomann, and E. C. Waymire, *Advection–Dispersion Across Interfaces*, Stat. Sci. **28** (2013), no. 4, 487–509, DOI 10.1214/13-STS442.

[48] J. Ramirez, E. Thomann, E. Waymire, J. Chastenet, and B. Wood, *A Note on the Theoretical Foundations of Particle Tracking Methods in Heterogeneous Porous Media*, Water Resour. Res. **44** (2007), W01501, DOI 10.1029/2007WR005914.

[49] J. M. Ramirez, *Skew Brownian Motion and Branching Processes Applied to Diffusion-Advection in Heterogenous Media and Fluid Flow*, PhD thesis, Oregon State University, 2007.

[50] J. M. Ramirez, E. A. Thomann, E. C. Waymire, R. Haggerty, and B. Wood, *A generalized Taylor-Aris formula and skew diffusion*, Multiscale Model. Simul. **5** (2006), no. 3, 786–801, DOI 10.1137/050642770.

[51] P. Salamon, D. Fernàndez-Garcia, and J. J. Gómez-Hernández, *A review and numerical assessment of the random walk particle tracking method*, J. Contaminant Hydrology **87** (2006), no. 3-4, 277–305, DOI 10.1016/j.jconhyd.2006.05.005.

[52] K. Semra, *Modélisation tridimensionnelle du transport d'un traceur en milieux poreux saturé: évaluation des théories stochastiques*, PhD thesis, Université Louis Pasteur, Strasbourg, 1994.

[53] G. Shorack and J. Wellner, *Empirical processes with applications to statistics*, John Wiley & Sons, 1986.

[54] D. Spivakovskaya, A. W. Heemink, and E. Deleersnijder, *Lagrangian modelling of multi-dimensional advection-diffusion with space-varying diffusivities: theory and idealized test cases*, Ocean Dynamics **57** (2007), no. 3, 189–203, DOI 10.1007/s10236-007-0102-9.

[55] D. Spivakovsakaya, A.W. Heemink, and E. Deleersnijder, *The backward Ito method for the Lagrangian simulation of transport processes with large space variations of the diffusivity*, Ocean Sci. **3** (2007), no. 4, 525–535.

[56] D.J. Thomson, W.L. Physick, and R.H. Maryon, *Treatment of Interfaces in Random Walk Dispersion Models*, J. Appl. Meteorol. **36** (1997), 1284–1295.

[57] G. J. M Uffink, *Analysis of dispersion by the random walk method*, Delft University, The Netherlands, February 6, 1990.

[58] M. Zhang, *Calculation of diffusive shock acceleration of charged particles by skew Brownian motion*, Astrophys. J. **541** (2000), 428–435.

[59] C. Zheng and G. Bennett, *Applied Contaminant Transport Modeling*, 2nd ed., Wiley-Interscience, 2002.